Universidade de Aveiro
2022

José Tiago Monteiro Fernandes

Exploration of optimisation solutions for a radiant floor system

Análise exploratória de soluções de otimização para um piso radiante

Universidade de Aveiro
2022

José Tiago Monteiro Fernandes

Exploration of optimisation solutions for a radiant floor system

Análise exploratória de soluções de otimização para um piso radiante

Dissertação apresentada à Universidade de Aveiro para cumprimento dos requisitos necessários à obtenção do grau de Mestre em Engenharia Mecânica, realizada sob orientação científica de Doutor Tiago Manuel Rodrigues da Silva, Investigador (nível 1) do Departamento de Engenharia Mecânica, da Universidade de Aveiro, e Doutor João Alexandre Dias de Oliveira, Professor Auxiliar do Departamento de Engenharia Mecânica, da Universidade de Aveiro.

Esta dissertação teve o apoio dos projetos UIDB/00481/2020 e UIDP/00481/2020 - Fundação para a Ciência e a Tecnologia; e CENTRO-01-0145 FEDER-022083 - Programa Operacional Regional do Centro (Centro2020), através do Portugal 2020 e do Fundo Europeu de Desenvolvimento Regional.

O júri / The jury

Presidente / President

Prof. Doutor Ricardo José Alves de Sousa
Professor auxiliar c/ agregação da Universidade de Aveiro

Vogais / Comitee

Doutor António José Pereira de Figueiredo
Investigador doutorado (nível 1), Universidade de Aveiro

Doutor Tiago Manuel Rodrigues da Silva
Investigador doutorado (nível 1), Universidade de Aveiro

agradecimentos / acknowledgements

Um agradecimento muito especial à minha família, nomeadamente aos meus pais por me terem ajudado em tudo o que puderam. A todos os meus amigos que estiveram comigo ao longo do meu percurso académico, percurso este que foi longo e cheio de memórias. À minha namorada, um especial apreço por me aturar e ajudar em tudo.
Agradeço também aos meus colegas de curso de Engenharia Mecânica que estiveram ao meu lado nesta jornada.
Por fim, um agradecimento aos meus orientadores João Oliveira e Tiago Silva pela disponilidade e ajuda neste processo.

keywords Climatization; Numerical Analysis; Thermal Comfort; Heating; Optimization; Energy

abstract The building sector is responsible for 36% of total energy consumption and this contributes to 40% of total carbon dioxide emissions. In the coming years, the construction sector will grow even more. This is why there has been a global interest in finding solutions to reduce the energy consumption of commercial, industrial and also residential buildings. In order to improve the comfort of buildings and closed spaces, the use of solutions and systems that promote the heating and cooling of these spaces is common. Radiant floor systems have quite a lot of potential to reduce energy consumption of buildings and consequently their carbon footprint. The objective of this dissertation is to optimize a radiant floor system. For this optimization, different ways and tools on how to achieve this are studied and applied in the system, identifying at the same time the parameters that determine its performance. Multiple examples of radiant floors were studied and analysed including the heating transfer phenomena involving them. An optimization model will be generated resorting to different objective functions, constraints and variables to recommend a solution with the best possible result. Using analytical equations, a parametric study was done using a reference radiant floor system structure with parameters previously defined. It was found that the distance between the piping and the surface of the system, tube spacing and thickness of the layers are the most important parameters when it comes to heat flux output. To perform numerical simulations, the Design Exploration process has been followed to efficiently carry out this study, using a module called DesignXplorer, part of the commercial software ANSYS. Local sensitivities were found where the same conclusions as before were stated. Using analytical equations and numerical simulations, resourcing to Excel and Ansys optimization algorithms respectively, some optimized solutions are presented and discussed.

palavras-chave

Climatização; Análise Numérica; Conforto térmico; Aquecimento; Optimização; Energia

resumo

O setor da construção é responsável por 36% do consumo total de energia e isso contribui para 40% das emissões totais de dióxido de carbono. Nos próximos anos, o setor de construção vai crescer ainda mais. Esta é a razão pela qual tem havido um interesse global para arranjar soluções para reduzir o consumo de energia de edifícios comerciais, industriais e também residenciais. Para melhorar o conforto térmico dos edifícios e espaços fechados, é comum a utilização de soluções e sistemas que promovem o aquecimento e arrefecimento desses espaços. Os sistemas de piso radiante têm bastante potencial para reduzir o consumo energético de edifícios e consequentemente reduzir a pegada de carbono dos mesmos. Este trabalho tem como objetivo otimizar um sistema de piso radiante. Para concretizar esta otimização são estudadas diferentes formas e ferramentas de como o conseguir e por fim a sua aplicação no sistema, identificando ao mesmo tempo, os parâmetros que determinam o seu desempenho. Neste trabalho foram analisados e estudados vários exemplos de pisos radiantes, e os processos de transferência de calor envolvidos nos mesmos. Um modelo de otimização foi desenvolvido recorrendo a diferentes funções objetivo, restrições e variáveis para recomendar uma solução ótima. Utilizando equações analíticas, foi feito um estudo paramétrico usando uma estrutura de sistema de piso radiante de referência com parâmetros previamente definidos. Verificou-se que a distância entre a tubulação e a superfície do sistema, o espaçamento entre tubos e a espessura das camadas são os parâmetros mais importantes quando se trata do fluxo de calor. Para realizar as simulações numéricas, seguiu-se o processo de Design Exploration para realizar este estudo de forma eficiente, utilizando um módulo denominado DesignXplorer, parte do software comercial ANSYS. As sensibilidades locais foram calculadas pelo software onde as mesmas conclusões de antes foram tiradas. Através de equações analíticas e simulações numéricas, usando algoritmos de otimização do Excel e do Ansys respectivamente, algumas soluções otimizadas são apresentadas e discutidas.

Contents

1 Introduction **1**
- 1.1 Framework . . . 1
- 1.2 Document Structure . . . 2

2 Theoretical Background **3**
- 2.1 Radiant Floor System . . . 3
- 2.2 Different Types of Radiant Floor Systems . . . 4
- 2.3 Advantages of a Radiant Floor System . . . 6
- 2.4 Disadvantages of a Radiant Floor System . . . 7
- 2.5 Hydronic Radiant Floor System Structure . . . 8
- 2.6 Heat Transfer . . . 9
  - 2.6.1 Heat Transfer by Conduction . . . 9
  - 2.6.2 Heat Transfer by Convection . . . 10
  - 2.6.3 Heat Transfer by Radiation . . . 11
- 2.7 Heat Transfer Processes Occurring in Radiant Floor Systems . . . 11
- 2.8 Thermal Mass . . . 11
- 2.9 Thermo-Active Building Systems . . . 12
- 2.10 The Optimization Process . . . 13

3 State of the Art **15**
- 3.1 General Radiant Floor Research Review . . . 15
- 3.2 Control Strategies . . . 18
- 3.3 Models of Radiant Heating Systems . . . 20

4 Analytic Setup **23**
- 4.1 Pipe Spacing Influence . . . 23
- 4.2 Heat Transfer Between Heated Fluid and Piping . . . 25
- 4.3 Analytic Radiant Floor System Evaluation . . . 30

5 Numerical Setup **37**
- 5.1 Ansys Optimization Process . . . 37
  - 5.1.1 Desing of Experiments (DOE) . . . 38
  - 5.1.2 Response Surface . . . 38
  - 5.1.3 Optimization of Design Points . . . 39
- 5.2 Ansys Optimization Algorithms . . . 39

5.3 Radiant Floor System Setup 40
5.3.1 Mesh Independence Test 41
5.3.2 Model Validation 43
5.3.3 Model Setup 43
5.3.4 Custom DOE 47
5.3.5 Local Sensitivities 47
5.4 Optimization 52
5.4.1 Adaptative Single-Objective 52
5.4.2 NLPQL 53
5.4.3 MISQP 53
5.4.4 Results Compilation 54

6 Final Remarks **61**
6.1 Conclusions 61
6.2 Future Work 62

Bibliography **65**

List of Tables

4.1 Values of the constant variables for spacing research. 24
4.2 Properties of the fluids. 26
4.3 Values of the constant variables for piping analysis. 27
4.4 Heat flux results for each fluid. 27
4.5 Values of the optimal solution. 30
4.6 Values of the constant variables for radiant floor system analysis. 32
4.7 Values of the optimal solution for a radiant floor system. 35

5.1 Capabilities of the response surface optimization methods available in Ansys software [Exploration 2013]. 40
5.2 Comparison of operating parameters of a floor heating system calculated according to EN 1264 and numerically with Ansys software. 44
5.3 Properties of the materials. 45
5.4 Values of the local sensitivities for the temperature probe maximum temperature. 48
5.5 Values of the local sensitivities for the maximum heat flux. 49
5.6 Candidate points proposed by Ansys software using ASO. 53
5.7 Candidate points proposed by Ansys software using NLPQL. 53
5.8 Candidate points proposed by Ansys software using MISQP. 54
5.9 Best points resulting from all algorithms. 55

6.1 Parameters of the best radiant floor system configuration. 62

Intentionally blank page.

List of Figures

2.1 Air heated radiant floor system [Richard Watson 2004]. 4
2.2 Electric radiant floor system [by Danfoss 2022]. 5
2.3 Radiant hydronic heating system [John Siegenthaler 2012] 6
2.4 Radiant floor heating curve [Woodson 2010]. 7
2.5 Heat transfer processes occurring in a radiant floor. 12

3.1 Effects of cover type on heating time [Sattari and Farhanieh 2006]. 16
3.2 Design chart for radiant floor heating panel with oak wood floor covering [Shin *et al.* 2015]. 17
3.3 Comparison between dry and wet radiant floor setups [Rüdisser 2017]. . . 18
3.4 Data Communication for MPC [Joe and Karava 2019]. 19

4.1 Section of the radiant floor heating panel with embedded pipes [Shin *et al.* 2015] 24
4.2 Effect of tube spacing on heat flux. 25
4.3 Effect of different piping parameters on heat flux. 28
4.4 Section of the radiant floor heating panel with embedded pipes [Zhang *et al.* 2012]. 30
4.5 Effect of different parameters on radiant floor heat flux. 33
4.6 Effect of different parameters on radiant floor heat flux. 34

5.1 Model of a floor heating according to the EN 1264 standard [Exploration 2013]. 41
5.2 Convergence of Heat Flux results. 42
5.3 Convergence of Temperature results. 42
5.4 Mesh of the circle with no refinement. 43
5.5 Mesh of the circle with refinement. 43
5.6 Radiant Floor System 2D model. 44
5.7 Radiant Floor System 2D meshed model. 45
5.8 Temperature Distribution of the Radiant floor system. 46
5.9 Heat Flux Distribution of the Radiant floor system. 46
5.10 Measurements of the radiant floor slab. 47
5.11 Sensitivities of the output parameters. 48
5.12 3D Response surface of the Temperature Probe Maximum Temperature. . 49
5.13 3D Response surface of Heat Flux Probe Maximum Total. 50
5.14 Variation of the surface temperature with respect to the thickness of the surface layer for different values of the thickness of the tubing layer. . . . 50
5.15 Variation of the surface heat flux with respect to the thickness of the surface layer for different values of the thickness of the tubing layer. . . . 51

5.16 Variation of the surface temperature with respect to the thickness of the tubing layer for different values of the thickness of the surface layer. . . . 51
5.17 Variation of the heat flux with respect to the thickness of the tubing layer for different values of the thickness of the surface layer. 52
5.18 Geometry of the ASO model. 55
5.19 Geometry of the NLPQL model. 55
5.20 Geometry of the MISQP model. 55
5.21 Temperature Distribution of the ASO Radiant floor system. 56
5.22 Temperature Distribution of the NLPQL Radiant floor system. 56
5.23 Temperature distribution of the MISQP radiant floor system. 57
5.24 Heat flux distribution of the ASO radiant floor system. 57
5.25 Heat flux distribution of the NLPQL radiant floor system. 58
5.26 Heat flux distribution of the MISQP radiant floor system. 58
5.27 Configuration of the optimized model. 59

Chapter 1

Introduction

1.1 Framework

The building sector is responsible for 36% of total energy consumption and this contributes to 40% of total Carbon Dioxide emissions [Agency 2018]. Over the next 40 years, the building sector will grow by nearly 230 billion square meters [Shukla *et al.* 2020]. That is the reason why there has been a spark of interest globally to reduce the energy consumption of commercial and industrial buildings and also residential housing. The combination of strategies such as improving the efficiency of Heating, Ventilation and Air Conditioning (HVAC) equipment and reducing the thermal demand of the house by improving envelope conditions, better control and introducing renewable energy technologies can achieve significant reduction of greenhouse gas emissions.
Due to the current global landscape where a lot of nations are fighting against global warming, energy efficiency is becoming a more relevant theme as time goes by. Additionally HVAC systems account for 27% of energy consumption and 45% of peak electrical demand in commercial buildings [Department of Energy *et al.* 2011]. The climatization of buildings is a common practice used to maintain the level of comfort required by society and because of those needs there is always room for new research to improve existing technologies and by doing that, reducing not only the cost of implementation but also energy consumption. Radiant floor heating is a system that has been developing as time goes by, it offers advantages but also disadvantages.

Radiant floor systems have been the subject of research within the field of space heating water-based radiant systems, presenting a potentially viable solution for space heating because they are suitable for integration with renewable energy sources and have the ability to create a comfortable thermal environment. The applicability of the individual system type depends on their location (floor, wall, or ceiling), the configuration of material layers, the configuration of the tubing within those layers and consequently the level of thermal mass. These characteristics are crucial when choosing the most suitable system for a specific situation such as the construction of a new building vs. retrofitting of an existing building, thermal storage vs. fast thermal response, and traditional vs. low-temperature renewable heat source.

Without appropriate building designs and efficient heating, ventilation, and air-conditioning systems, large space buildings exhibit poor thermal comfort and high energy use. Due to the large differences in the construction, geometry, glazing, usage and location, there is no perfect size or solution and each building needs to be considered

independently for devising optimum solutions for creating a suitable indoor climate and saving energy of HVAC systems.

This dissertation was conducted in order to define the most important variables to take into account in the early stages of designing a radiant floor system, after defining those variables, optimization methods using 1D analytical equations and 2D numerical simulations will be applied to get the optimal solution using heat flux and surface temperature as the analysed outputs of the system.

Additionally, as stated before there is no perfect size or parameters to be applied in every situation, due to this each situation has to be analysed individually, with the work being done and evaluated in this dissertation, given specific constrains the model can be optimized for a certain output and that output can also be defined. An example of the usage of this can be a room that has heating demands of $50W/m^2$, with geometrical constrains such as the thickness of the layers the optimal positioning of the tubing to achieve the desired output can be found at the early design stage of the system, this helps with predicting the output and getting the best solution with the given constrains. Optimization consists in finding the best solution or highest achievable performance under given constraints. This concept has been widely applied to the most different areas of engineering, from the design of automobile components to the study of water networks.

1.2 Document Structure

Setting aside the current chapter, which contains the introduction and intentions of this work, the remainder of this dissertation is divided into 5 chapters. To assist the reader in accessing the content within, this document was organized with the following structure:

- Chapter two — Contains the background for this work, and provides the theoretical basis to have sensitivity and analyse correctly the phenomenons taking place in a radiant floor system.
- Chapter three — Presents a literature review, of what has been studied, what is being studied and what can be further studied. Taking into account the experiments analysed and studied, the most important variables are found when it comes to the performance of the radiant floor system.
- Chapter four — An analytical study is done using simplified 1D heat transfer equations. The influence of the studied parameters are analysed to evaluate which ones have the most effect on the heat flux output and to finalize, using Excel solver, an optimization is performed to find the optimal solution under certain constraints.
- Chapter five — Using Ansys® software, a 2D section of a radiant floor system is developed. After the mesh, calibration and validation of this model, using Ansys Design Explorer, optimization of the model is conducted using different methods.
- Chapter six — Contains the critical conclusions and discussion of the previous chapters along with the final comments on the dissertation and the results.

Chapter 2

Theoretical Background

Hydronic heating systems operate with moderate chilled or hot water temperature so the efficiency of the system is higher, reducing the use of energy resources. Typical radiant floor systems are embedded in concrete slabs offering significant potential for load shifting, e.g. pre cooling during the summer, due to thermal mass. This approach enables cost benefits due to the high chiller efficiency and low electricity price at night. These benefits can be maximized with prediction-based optimal control. Previous research also report challenges associated with the control of radiant systems due to their large thermal inertia that is difficult to handle with conventional control strategies to respond to sudden changes in weather or room temperature. The low heating and cooling power determined by the supply-water temperatures to overcome condensation and discomfort constraints cause additional limitations [Verbeke and Audenaert 2018].

2.1 Radiant Floor System

Radiant floor heating systems have existed for quite some time. The origins of these systems can be traced back to the Roman Empire, the Romans heated their floors using exhaust gases from wood fires directed towards open space under raised floors [Woodson 2010]. Nowadays radiant floor systems mainly use water as the transfer fluid or can consist of electric resistances throughout the floor. Each type of panel is applied according to the place it is going to be applied to and the purpose it has. Hydronic radiant panels can receive fluid from practically any source projected towards water heating, such as heat pumps, boilers and even using renewable energy sources.

A hydronic radiant panel is any object warmed by passing heated water through tubing embedded in or attached to it, and which releases at least 50% of that heat to its surroundings as thermal radiation [John Siegenthaler 2012]. The heated water is simply the material used to deliver heat to a Hydronic radiant panel. If a heating cable was embedded in or attached to the same object, one could refer to it as an electric radiant panel. Once heat has been transferred to the materials that make up the radiant panel, its shape, orientation, surface temperature, surface properties, and surroundings determine its thermal output.

Radiant systems installed on the floor account for over 90% of all hydronic radiant panel installations [John Siegenthaler 2012]. However, radiant panel heating is not limited to floors. There are several established methods of incorporating hydronic tubing

into walls and ceilings [Liu *et al.* 2015].

2.2 Different Types of Radiant Floor Systems

There are 3 types of radiant floor systems that are currently used or were more commonly used in the past.
The first example is an air heated radiant floor system (Figure 2.1), which involves the production of hot air and its distribution throughout the piping embedded in the radiant floor. This system can work in a closed circuit or also by having ambient air supplied to it, forcing its circulation through the pipes. This type of system has been developed for different types of construction utilizing the floor, the ceiling or even both [Richard Watson 2004].

[Bozkir and Canbazoğlu 2004] confirmed that an air heated system has less heating efficiency than a hydronic system but can be an alternative if there is a need to reuse a hot air source already existent in the building. This system has a satisfactory performance in mild climates and in houses with good thermal insulation, even though it does not have the same heating capabilities as other systems it has the same benefits with more heating quality and comfort when compared to direct air heating systems.

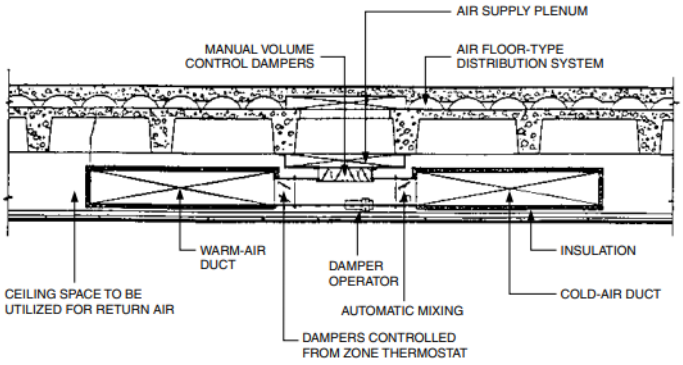

Figure 2.1: Air heated radiant floor system [Richard Watson 2004].

The second type of system is an electric radiant floor system (Figure 2.2), it uses electricity to directly heat up the electric resistances present on the floor. One of the advantages of this type of system is the fact that it does not require a lot of components and infrastructure that other systems need, making it an easier installation and a more economical option. It requires no boiler or plumbing required as there is in hot water hydronic systems which means fewer safety risks and lower repair costs overall. It is easy to retrofit or install as part of any renovations. You can easily fit an under-floor heating system as part of a bathroom renovation, or under a bedroom carpet, without affecting any existing heating systems.

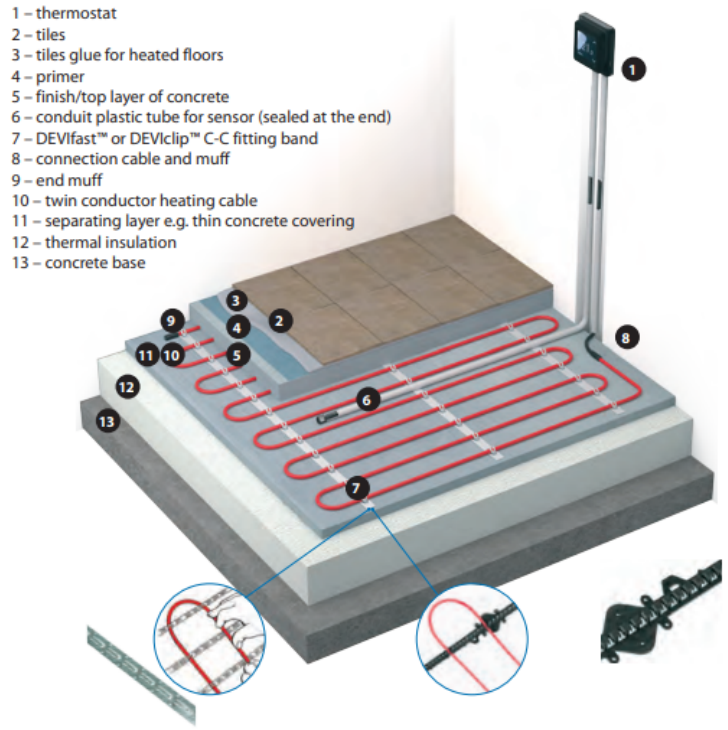

Figure 2.2: Electric radiant floor system [by Danfoss 2022].

The third and last system is a hydronic one (Figure 2.3). Hydronic heating systems use water (or water-based solutions) to move thermal energy from its source to where it is required. The water flowing through the system is neither the source of the heat nor its destination, only its means of transportation. Thermal energy is absorbed by the heat source, conveyed by the water through the distribution system and finally released in a heated space by a heat emitter. Water contains a lot of characteristics that make it ideal for this type of application, it is widely available, nontoxic, nonflammable and has one of the highest heat storage abilities of any fluid. Modern piping materials in hydronic heating systems include copper tubing and cross-linked polyethylene tubing (PEX). Another type of tubing sometimes used is polibutylene (PB) tubing. Copper tubing is the most popular type of piping used for general convection heating, such as systems utilizing baseboard heating elements, kick-space heaters and space heaters. PEX tubing is most often used for radiant floor heating systems. Since copper expands and contracts with temperature variations, the tubing must be supported properly to maintain a quiet heating system. PEX tubing is a polymer (plastic) material. It is sold in long coils, and suitable for many hydronic applications. Standard PEX tubing can handle water with a temperature of 180°C. Both copper and PEX tubing have their place in heating systems. There is a common rule to use copper tubing for general heating applications and to use PEX for radiant floor heating.

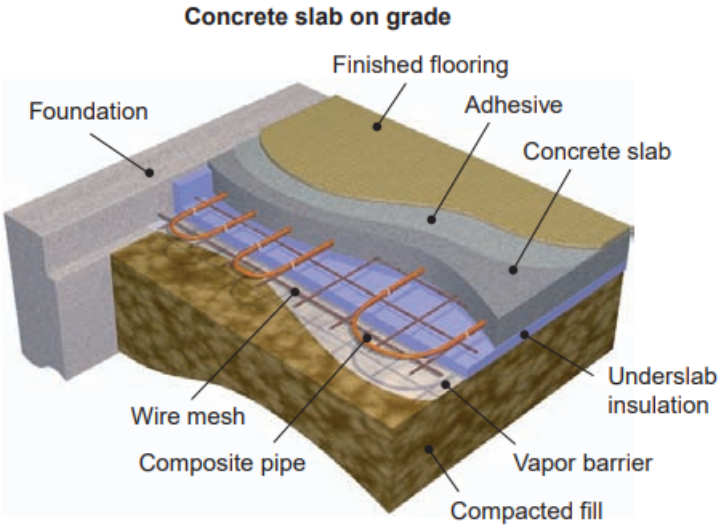

Figure 2.3: Radiant hydronic heating system [John Siegenthaler 2012]

2.3 Advantages of a Radiant Floor System

Compared to traditional forced heating systems or even baseboard heating systems, radiant heating has many advantages and benefits, including the following [John Siegenthaler 2012]:

- A system that delivers great comfort. The majority of people with the opportunity to compare the comfort offered by a properly installed radiant panel heating system will state that it is more comfortable than other methods of heating, as depicted in Figure 2.4.
- A system that is out of sight. Not a lot of people enjoy looking at chunks of a heating system that, out of necessity, are located within an occupied space. In contrast most radiant panels are incorporated into the building and are totally located within floor, walls or ceilings [John Siegenthaler 2012].
- A system that is extremely durable. Due to radiant panels being built into the structure, they are usually well protected from physical damage.
- A system with little operating noise. A correctly designed and installed radiant panel system operates silently. Modern heat sources and circulators operate with minimal noise and are usually located in a specific room.
- A system that is compatible with low-temperature heat sources. Many types of radiant panels can operate at relatively low water temperatures. This allows low-temperature heat sources such as solar collectors and condensing boilers to supply heat while operating at relatively high efficiency.
- A system with thermal storage. Some hydronic radiant panels, such as a heated concrete floor slab has a high thermal mass. These types of panels can store large quantities of heat, allowing them to deliver a surge of heat in situations where there is a sudden change on the interior conditions.

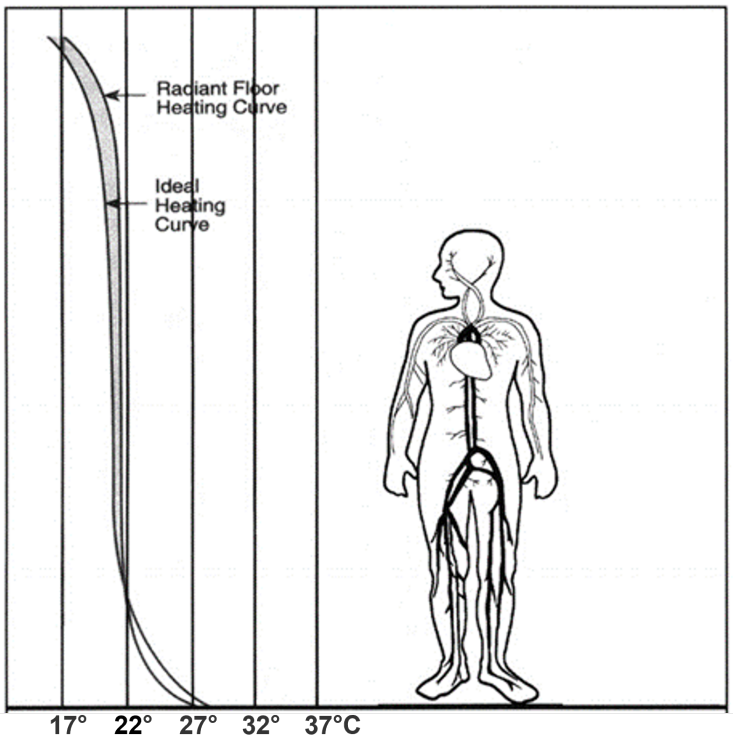

Figure 2.4: Radiant floor heating curve [Woodson 2010].

- Some systems are adequate for a fast response. Not every hydronic radiant panel has a high thermal mass. Some are specifically designed for low thermal mass giving them a quick response. Radiant walls and ceilings are usually of lower thermal mass construction, and well suited for situations where comfort needs to be quickly established after a prolonged temperature setback period.

- A system that is easily zoned. It can easily be configured for room-by-room zoning. Sleeping areas can be maintained cool while bathrooms are maintained warm.

2.4 Disadvantages of a Radiant Floor System

Despite all the advantages there are some drawbacks that are important to consider before making the investment, such as:

- Challenges associated with the control of radiant systems due to their large inertia that is difficult to handle with conventional control strategies in order to respond to abrupt changes in weather or room temperature [Joe and Karava 2019].

- Higher installation cost when compared to other heating systems [Woodson 2010].

- Since the installation is done permanently and is integrated into the building, the removal or substitution of the piping due to maintenance is difficult.

2.5 Hydronic Radiant Floor System Structure

Radiant floors are made up of layers of different materials. The layers have different contributions to the operation of the underfloor heating system, which can be more or less favorable, depending on the characteristics of the materials that constitute each one. The floor structure of radiant floor systems is a typical composite multilayer, as shown in Figure 2.3. There are usually three layers from the top to the bottom of the floor, that is, surface, filling, and insulating layers. Heated water is supplied by embedded circular pipes in the filling layer. The surface is the top layer of the pavement, and it is through this layer that energy is conveyed to the indoor environment by convection and radiation. This energy is transferred to it by the filling layer that is under it. In the filling layer, the pipe through which the hot water circulates is incorporated, and its main objective is to store the thermal energy transmitted to it by the water in the pipe. To prevent the loss of thermal energy to non-climatized spaces, an insulating layer is placed below the filling layer.

Surface Layer

The underfloor heating system is compatible with all types of floor surface materials. The thickness and thermal conductivity are the parameters with the most importance when analysing the system because through these values it is possible to study the thermal contribution of this layer.

Filling Layer

The filling layer incorporates the piping circuit, and plays an important role in the thermal performance of the floor because it stores the heat that is transferred to it by the fluid that circulates in the tubes, to then transmit it to the surface. Thus, the thickness of this layer is a parameter to which attention should be paid in the design phase of the flooring system, since the thermal inertia of the system increases as the thickness of it increases. On the other hand, very small thicknesses can jeopardize the structural resistance of this layer.

Insulating Layer

Thermal insulation is integrated into the underfloor heating system to prevent heat flux into non-air-conditioned spaces. Materials that have thermal conductivities lower or equal to 0.065 W/m.°C are considered thermal insulating materials [Akçaözoğlu *et al.* 2013]. Expanded polystyrene (EPS), rock wool and extruded polystyrene (XPS) are the types of materials commonly used as insulation in underfloor heating systems.

Tubing

Tubing in underfloor heating systems must have some flexibility and a good behavior at high temperatures, and, therefore it is most of the time achieved by using PEX tubing. Consulting the catalogs of some manufacturers of underfloor heating systems, the diameters of the tubes used in these systems normally range between 14 mm and

20 mm, in addition to the dimensions of the pipes where the water circulates, the spacing between these tubes is also a parameter to pay attention to.

2.6 Heat Transfer

In general, heat transfer describes the flow of heat (thermal energy) due to temperature differences and the subsequent temperature distribution and changes. The study of transport phenomena concerns the exchange of momentum, energy, and mass in the form of conduction, convection, and radiation.

2.6.1 Heat Transfer by Conduction

Heat conduction can be seen as the transfer of energy from the particles with most energy to the ones with least energy inside a substance due to the interactions between particles. This way, the exchange of energy is directed from the high temperature region to the one with low temperature, by kinetic motion or by direct impact of molecules in the case of fluids or by the motion of electrons in the case of solid materials.

On microscopic scale, heat conduction occurs as hot, rapidly moving or vibrating atoms and molecules interact with neighboring atoms and molecules, transferring some of their energy (heat) to these neighboring particles. In other words, heat is transferred by conduction when adjacent atoms vibrate against one another, or as electrons move from one atom to another. Conduction is the most significant means of heat transfer within a solid or between solid objects in thermal contact. Fluids— especially gases—are less conductive. Thermal contact conductance is the study of heat conduction between solid bodies in contact. Steady state conduction is a form of conduction that happens when the temperature difference driving the conduction is constant, so that after an equilibration time, the spatial distribution of temperatures in the conducting object does not change any further. In steady state conduction, the amount of heat entering a section is equal to amount of heat coming out.

Fourier´s Law

The basis of conduction heat transfer is Fourier´s Law. This law involves the idea that the heat flux is proportional to the temperature gradient in any direction n. Thermal conductivity, k, a property of materials that is temperature dependent, is the constant of proportionality.

$$q_k = -kA\frac{\partial T}{\partial n} \tag{2.1}$$

Where
q is the thermal flux
k is the thermal conductivity of the material [W/ (m K)]
A is the surface area of the heat being transferred [m^2]
T is the temperature [K]

For many simple applications, Fourier's law is used in its one-dimensional form. In the x-direction.

$$q_x = -k\frac{\partial T}{\partial x} \tag{2.2}$$

Transient conduction occurs when the temperature within an object changes as a function of time. Analysis of transient systems is more complex and often calls for the application of approximation theories or numerical analysis by computer. The heat equation is a parabolic partial differential equation which describes the distribution of heat (or variation in temperature) in a given region over time. For a function *u(x,y,z,t)* of three spatial variables *(x,y,z)* (see cartesian coordinates) and the time variable t, the heat equation is:

$$\frac{\partial u}{\partial t} - \alpha\left(\frac{\partial^2 u}{\partial x^2} + \frac{\partial^2 u}{\partial y^2} + \frac{\partial^2 u}{\partial z^2}\right) = 0 \tag{2.3}$$

2.6.2 Heat Transfer by Convection

Heat convection occurs when bulk flow of a fluid (gas or liquid) carries heat along with the flow of matter in the fluid. The flow of fluid may be forced by external processes, or sometimes by buoyancy forces caused when thermal energy expands the fluid, thus influencing its own transfer. The latter process is often called "natural convection". All convective processes also move heat partly by diffusion, as well. Another form of convection is forced convection. In this case the fluid is forced to flow by use of a pump, fan or other mechanical means.

Newton´s Law of cooling

Convection-cooling can sometimes be described by Newton's law of cooling in cases where the heat transfer coefficient is independent or relatively independent of the temperature difference between object and environment. This is sometimes true, but is not guaranteed to be the case. Newton's law, which requires a constant heat transfer coefficient, states that the rate of heat loss of a body is proportional to the difference in temperatures between the body and its surroundings. The rate of heat transfer in such circumstances is derived below. Newton's cooling law is a solution of the differential equation given by Fourier's law:

$$\frac{\mathrm{d}Q}{\mathrm{d}t} = h \cdot A \cdot (T(t) - T_{\mathrm{envi}}) = -h \cdot A \cdot \Delta T(t) \tag{2.4}$$

Where
Q is the thermal energy
h is the heat transfer coefficient [W/ $\left(\mathrm{m}^2\ \mathrm{K}\right)$]
A is the surface area of the heat being transferred [m^2]
T is temperature of the objects surface and interior [K]
T_{envi} is the temperature of the environment [K]

The heat transfer coefficient h depends upon physical properties of the fluid and the physical situation in which convection occurs.

2.6.3 Heat Transfer by Radiation

Thermal radiation is energy emitted by matter as electromagnetic waves, due to the pool of thermal energy in all matter with a temperature above absolute zero. Thermal radiation propagates without the presence of matter through the vacuum of space. Thermal radiation is a direct result of the random movements of atoms and molecules in matter. Since these atoms and molecules are composed of charged particles (protons and electrons), their movement results in the emission of electromagnetic radiation, which carries energy away from the surface. Emissive power of a surface:

$$E = \sigma \cdot \varepsilon \cdot T_{\mathrm{s}}^4 \tag{2.5}$$

Where
ε is emissivity, which is a surface property ($\varepsilon = 1$ is a black body).
σ is Steffan Boltzman constant $= 5.67 \cdot 10^{-8} \mathrm{W/m^2K^4}$
T_{s} is absolute temperature of the surface [K]

The above equation is derived from Stefan Boltzmann law, which describes a gross heat emission rather than heat transfer. The expression for the actual radiation heat transfer rate between surfaces having arbitrary orientations can be quite complex. However, the rate of radiation heat exchange between a small surface and a large surrounding is given by the following expression:

$$q = \sigma \cdot \varepsilon \cdot A \cdot \left(T_{\mathrm{s}}^4 - T_{\mathrm{sur}}^4\right) \tag{2.6}$$

Where
T_{sur} is the absolute temperature of the surroundings [K].

2.7 Heat Transfer Processes Occurring in Radiant Floor Systems

Radiant floor systems involve the three different heat transfer mechanisms, convection within pipes, conduction within layers, and radiation/convection between floor surface and indoor environment. Water is supplied by the embedded parallel circular pipes in the filling layer. Firstly, there is heat exchange between water and the internal surface of the pipes, then heat conduction occurs within the pipes' wall and layers of floor, at last the floor surface will exchange heat with the indoor environment by convection and radiation. The amount of transferred heat through radiation and convection from the surface material depends on a lot of parameters such as the surface material properties, indoor air temperature, air movement, building insulation, occupants, floor cover, and less on outside weather conditions. Radiation occurs between the floor surface and inner surfaces of envelopes, and convective heat exchange occurs between the floor surface and the indoor air. A scheme of these processes can be seen in Figure 2.5.

2.8 Thermal Mass

For transient analysis the heat storage in materials must be taken into account. The 1D heat conduction equation without internal heat generation is showed in Equation 2.7.

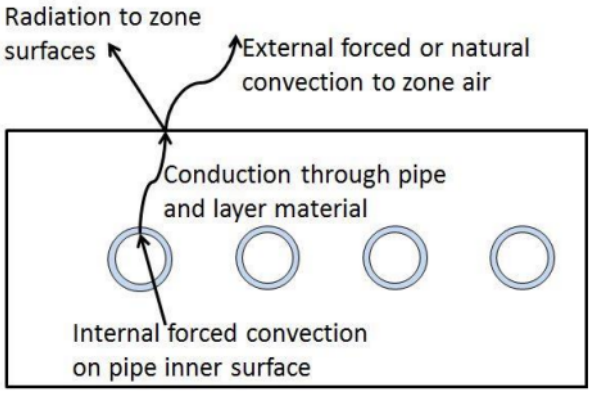

Figure 2.5: Heat transfer processes occurring in a radiant floor.

With the assumption of a temperature independent conductivity of the material, Equation 2.7 is rewritten to Equation 2.8.

$$\rho C_p \frac{\partial \theta}{\partial t} = \frac{\partial}{\partial x} \mathrm{k} \left(\frac{\partial \theta}{\partial x} \right) \tag{2.7}$$

$$\frac{\partial \theta}{\partial t} = \alpha \frac{\partial^2 \theta}{\partial x^2} \tag{2.8}$$

α is the thermal diffusivity of a material. It reflects the ability of the material to lead temperature and is equal to conductivity divided by the specific heat capacitance and density. These three parameters affect how the temperature changes over time within a material that experiences heat conduction. With a low conductivity and high heat capacitance the temperature will change slowly over time. The opposite are materials of high conductivity and low heat capacity. One good example of this is aluminum, which quickly becomes warm and leads heat very well. Thin sheets of Aluminum are hence frequently used in hydronic radiant underfloor heating to diffuse the temperature evenly over the surface.

2.9 Thermo-Active Building Systems

Related to the themal mass of building there is a type of building called thermo-Active Building Systems (TABS) which are a system where the thermal mass of the Radiant Heating System is significant. It can be water tubes embedded in the concrete slab of a building or in a concrete layer inside the building. The main point is that the thermal mass affects the thermal performance of the system significantly. A high heat capacity leads to a slow temperature change of a material and TABS will thus react slowly to sudden changes in load. Rapid changes in load conditions might be tough to meet because of this. In such an environment it is necessary an additional fast responsive heating system to aid the TABS. This secondary system also becomes necessary at high loads because TABS does not have a high heating capacity due to its low surface temperature. Research shows that TABS have a self-regulating property because of its thermal mass, thus dampening the peak temperature oscillations. This is analogous to coastal climates that are cool in the summer and mild in the winter because of the high

heat capacity of the ocean. Because it only handles the sensible load there is always a need for an air system to take care of the latent load. For modern buildings with super insulated envelopes TABS has been found to be especially promising considering thermal efficiency and comfort [Park *et al.* 2014]. It is also expected that with the progress of predictive control strategies TABS have good prospects for new constructions in the future. If room temperature level needs to be changed during the day, the thermal inertia of the systems is important. Due to the thermal mass of the radiant structure, the continuous operation with a water temperature that is too low or too high can result in under-cooling or over-heating problems [Olesen 2012]. In addition, the high thermal inertia of TABS can often cause difficulty in the control; different comfort requirements of the different rooms included in the same hydraulic zone, the need for manual switching between the heating and cooling mode and unnecessarily high energy consumption for water circulation [Gwerder *et al.* 2008].

2.10 The Optimization Process

The definition of optimization is dependent on the objective for which the optimization is used for. Generally, the act of optimizing something may translate into restructuring it with the objective of obtaining the highest possible efficiency or the determination of the solution that, among all possible solutions, leads to the most satisfactory results.

In a more technical way, optimization is said to be the process of maximizing or minimizing the required objective function while certain constraints are satisfied. For technology engineers to apply optimization methods to a project, they need to have a detailed understanding of both theory and algorithms and their specific techniques. This is due, first of all, to the fact that considerable effort is needed to apply optimization techniques to practical problems to achieve an improvement in the performance of the studied product. Because of this, maybe, optimization has been used, in particular, to help the projection process, namely to support decision-making, not to develop concepts, or to develop a detailed project. In all optimization problems, the intended purpose is always qualified by the words, minimize, decrease, maximize. All these and many more similar words can be substituted by the word optimal. What is intended may be called an objective. If this objective can be transcribed by a mathematical equation, it takes the name of objective function. Additionally, all these objectives must satisfy certain conditions for it to be acceptable. These conditions are called project constraints.

Terms used in optimization include design variables, design parameters and design functions. These are used to create the objective function and constraints.

An example of an optimization problem can be seen as following:

$$\text{Find}\,\mathbf{x} = \begin{bmatrix} x_1 \\ x_2 \\ \vdots \\ x_n \end{bmatrix} \text{ which minimizes } f(\mathbf{x}) \tag{2.9}$$

subjected to the following constraints,

$$g_j(\mathbf{x}) \leq 0, \quad j = 1, 2, \cdots, m \tag{2.10}$$

$$h_k(\mathbf{x}) = 0, \quad k = 1, 2, \cdots, l \tag{2.11}$$

$$x_i^{\min} \leq x_i \leq x_i^{\max}, \quad i = 1, 2, \cdots, n \tag{2.12}$$

where $\mathbf{x}$ is the n-dimensional vector of design variables (or vector of project), f($\mathbf{x}$) is the objective function, and $g_j(\mathbf{x})$ and $h_k(\mathbf{x})$, are defined as constraints of (non-strict) inequality and equality, respectively. The last constraints can be called simple constraints or side constraints.

Project Varibables

$$\mathrm{x} = \left[\begin{array}{cc} x_1 & x_2 \dots x_n \end{array} \right]^{\mathrm{T}}$$

They are entities that define a project, a particular design, a procedure or a control because they are the set of variables that establish a specific solution. They can be continuous, discreet or integer. The space of dimension n is called space of design variables or domain of variables. The variables must be independent (amongst them).

Objective Function

The optimal solution is found due to a specific objective from a project, however, subject to certain limitations. The objective function is identified and expressed mathematically through a function (or a set of functions).

Constraints

Project variables can´t be chosen at random. They have to satisfy certain and determined functionalities and specific requirements. These are called constraints.

Chapter 3

State of the Art

3.1 General Radiant Floor Research Review

The radiant floor heating panel should be designed to maintain the indoor condition within the comfort range, to prevent occupant discomfort when contacting floor surfaces of uneven temperature distribution, and to prevent skin burn and unwanted deformation of materials [ISO 2012]. To maintain the indoor condition within the comfort range [Alfano *et al.* 2014], heat flux from the floor surface should be sufficient to deal with the heating load. To prevent occupant discomfort due to contact with uneven floor surface temperatures, the difference between maximum and minimum floor surface temperature (DFST) needs to be as small as possible. In order to prevent skin burn and unwanted deformation of materials, the maximum floor surface temperature (MFST) needs to be lower than a specific value, depending on the floor covering materials [ISO 2012]. The human body usually is in direct contact with the floor surface, and to prevent local discomfort, the indoor thermal environment of radiant heating system needs to be considered [Rhee *et al.* 2017]. The floor surface temperature and heat transfer are the key parameters that should be taken in control of radiant floor heating systems [Wu *et al.* 2015]. According to ASHRAE 55 and ISO 7730 [ISO 2005], the field temperature depends on the floor surface composition and the cultural life style of occupants, if they are standing and wearing shoes or not, the surface temperature is recommended to be between 19 and 29°C for cooled and heated spaces, respectively.

Hasan et al. [Hasan *et al.* 2009] analyzed, by using dynamic simulation, the performance of a low temperature water heating system used in an apartment. Parameters such as the indoor air temperature and human thermal comfort are compared with classical systems: floor heating systems and radiator. The influence of the vertical difference of air temperature has been evidenced via experiments in a test room and it was concluded that there is only a small difference inside the test room not resulting in a singnificant thermal discomfort.

Laouadi [Laouadi 2004] developed a model for analyzing radiant heating and cooling systems which can be used in building energy simulation software, the model targets energy simulation software that uses one-dimensional numerical modeling to calculate heat transfer withing the building construction assemblies. Weitzmann et al. [Weitzmann *et al.* 2005] developed a two-dimensional dynamic model for simulation of floor heating systems. Using this model they calculated the heat loss value and the temperature of a slab on a grade floor with floor heating system in which it was concluded that the foun-

dation has a large influence on the energy consumption and heat loss to the ground. Jin et al. [Jin *et al.* 2010] proposed a calculation method for the floor surface temperature in radiant floor heating/cooling systems which is helpful to design the radiant floor system and estimate the heating/cooling capacity of the system. Sattari and Farhanieh [Sattari and Farhanieh 2006] studied the effects of design parameters such as pipe diameter, type (material), number, thickness and cover of the system on the performance of a typical radiant floor heating system using finite element method. An example of this can be seen in Figure 3.1 where the time to reach the desired temperature was calculated using different types of covers, it was concluded that materials with a higher conductivity take less time to heat up. The triangles represent the curve with wood, the squares the curve with concrete and the rhombus with steel.

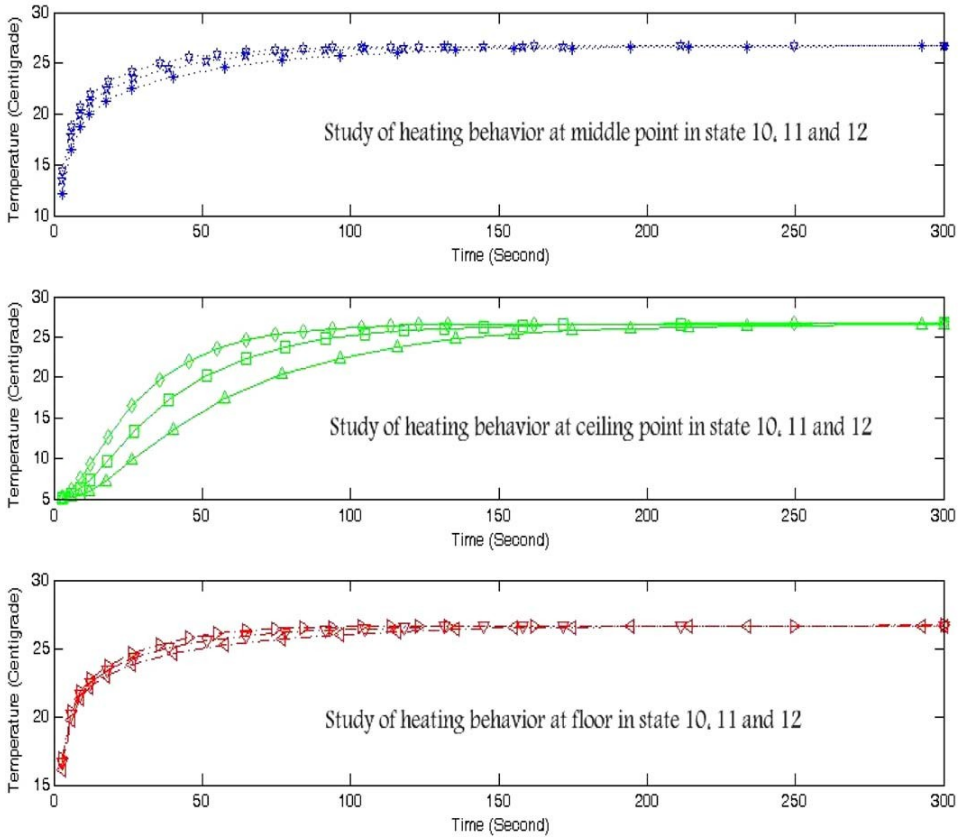

Figure 3.1: Effects of cover type on heating time [Sattari and Farhanieh 2006].

Current design convention focuses mainly on securing enough heat flux and not a lot of attention is given to floor surface temperature distribution. This is where a study conducted by Shin et al. [Shin *et al.* 2015] analyzed the floor surface temperature distribution of the radiant floor heating panel conducting numerical simulations and proposed design charts to predict heat flux, maximum surface temperature and difference between maximum and minimum surface temperature were developed, as shown in Figure 3.2. It is done to provide researchers with the option to evaluate a number of radiant floor options at the same time.

The most popular type of radiant floor is floor heating using wet technology, also

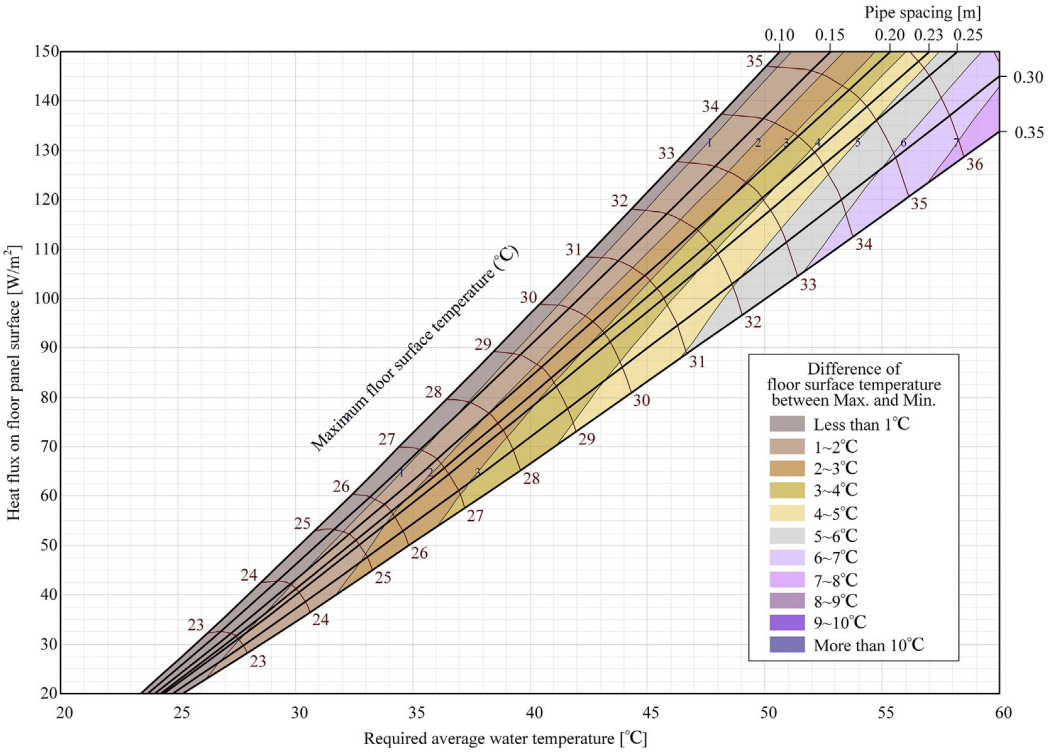

Figure 3.2: Design chart for radiant floor heating panel with oak wood floor covering [Shin *et al.* 2015].

known as a heavyweight system. A scheme of this system is shown in Figure 3.3a, in which the heating pipe is embedded in the screed layer. Wet setup is most often chosen during the construction of buildings, when it is possible to lay pipes on a layer of thermal insulation, before making the screed. Wet floor heating systems are considered difficult to regulate. Due to the high thermal inertia, it is not possible to cool down quickly when the room temperature is too high [Zhou *et al.* 2018]. This disadvantage of the wet system can be reduced by the use of lightweight systems, also called dry systems. A scheme of this system can be seen in Figure 3.3b.
Dry systems have even up to 6 times shorter time of heating up and cooling down than wet systems [Zhao *et al.* 2014].

Thomas et al. [Thomas *et al.* 2011] found that lightweight floor heating reaches 80% of its power after 30 min from the start of operation. In dry systems, the heating pipe is not immersed in the screed layer, but is placed over the thermal insulation layer. The plate, most often made of EPS, is profiled, the size of the channels is adjusted to the outer diameter of the pipe. In order to increase the thermal efficiency, the insulation layer is covered with a radiant sheet, made of aluminium or metallized polyethylene [Werner-Juszczuk 2018].

Qiu and Li [Qiu and Li 2011] compared the temperature distribution on the surface of a radiant floor made in a dry and wet system. Pipes were installed in a profiled board, covered with an aluminium radiant sheet of unknown thickness. The dry radiant floor was characterized by less distribution uniformity (surface temperature amplitude up to 4.64°C for mean water temperature of 45°C) than wet (surface temperature amplitude

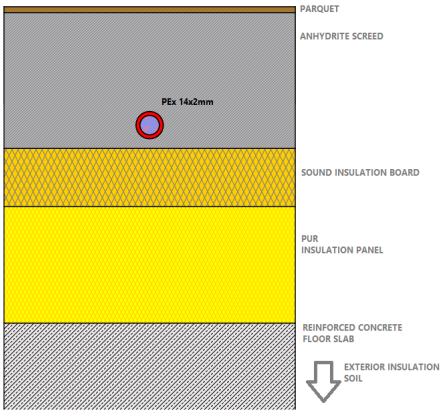

(a) Underfloor heating dry setup [Rüdisser 2017].

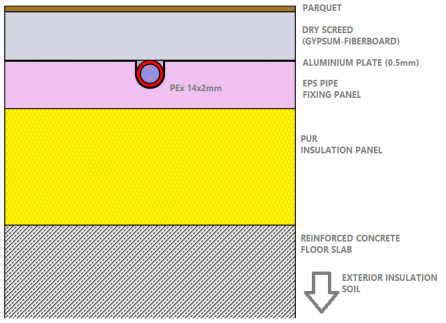

(b) Underfloor heating wet setup [Rüdisser 2017].

Figure 3.3: Comparison between dry and wet radiant floor setups [Rüdisser 2017].

up to 1.69°C for mean water temperature of 45°C).

Zhang et al. [Zhang *et al.* 2013] investigated the effect of pipe spacing and water temperature on the performance of lightweight floor heating. It was concluded that the higher the water temperature and the smaller pipe spacing, the higher dry floor heating efficiency. The construction, which was tested numerically and experimentally, consisted of pipes laid on a non-profiled heat-insulated board, covered with aluminium foil of unknown thickness. The pipes were placed in the air layer formed by the keel that supported the surface layer. An uneven temperature distribution was observed on the surface of the floor heating.

Bojic et al. [Bojić *et al.* 2013] presented the energy, environmental and economic results of research on the performance of floor, wall and ceiling heating. The results of this study showed that by heating the floor and ceiling at the same time, ie. by using floor ceiling panels they achieve the best results taking into account the previously mentioned indicators. On the other hand, the worst results were achieved with the use of ceiling panels.

3.2 Control Strategies

An important aspect of radiant floor systems is the control of the system itself. There have been multiple studies done with different ways to control it. In the most recent review on the control of TABS, Romani et al. [Romaní *et al.* 2016] classified the control strategies into on/off criteria (including night operation and intermittent operation), supply temperature control, pulse width modulation, model predictive control, adaptive control, and gain scheduling control. Among the control strategies, the supply temperature control with heating and cooling curves was reported as the most common for most TABS controls [Romaní *et al.* 2016]. The basic system that is currently used is just a switch that turns on/off [Romaní *et al.* 2016]. There is another model of control that is done by changing the supply temperature, where the supply water is continuously regulated according to the outdoor temperature, another variable that can be used is accounting the uncertainties in internal and solar heat and gains throughout the

day [Romaní *et al.* 2016]. Another type of control is called Pulse width modulation (PWM) which is a special case of intermittent operation ON/OFF control in the sense that pumps are frequently turned off to allow heat to accumulate on the surface for faster removal of heat when pumps are turned back on [Schmelas *et al.* 2015]. There is also a control type called gain scheduling control (GSC), which exists to handle the variations of heat gain during the system operation. In this approach, non-linear systems are divided into piecewise linear regions with different heat gains, and for each region, a linear proportional-integral-derivative (PID) is used [Romaní *et al.* 2016]. Another study presented a Model-Predictive Control (MPC) strategy to optimize the performance of hydronic radiant floor systems. It uses dynamic estimates and predictions of zone loads and temperatures, outdoor weather conditions, estimated occupancy levels and HVAC system models to minimize energy consumption and cost. This is all done meeting equipment and thermal comfort constraints [Joe and Karava 2019], a scheme of this process can be seen in Figure 3.4.

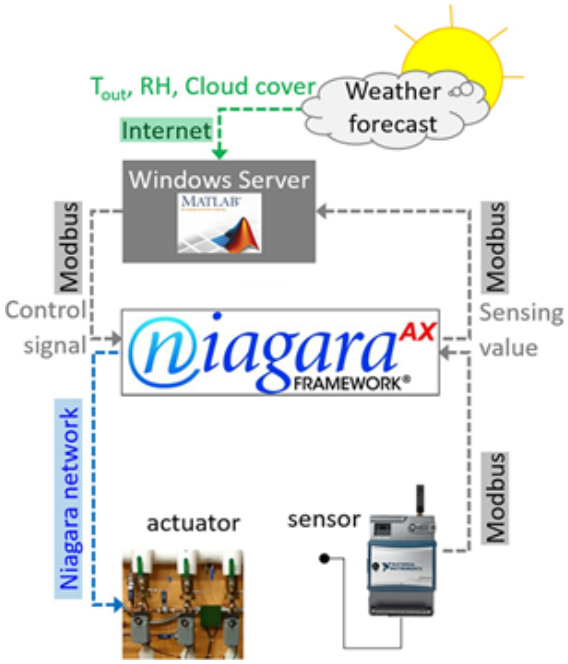

Figure 3.4: Data Communication for MPC [Joe and Karava 2019].

It was concluded that in the cooling season, the cost savings of the radiant floor system with MPC are about 34% compared to the simulated feedback control for the same system. In heating season, the energy savings are about 16% when compared to the feedback control [Joe and Karava 2019]. A major share of saved energy when using MPC systems comes from the intermittent operation of circulation pumps, with savings up to 81% [Schmelas *et al.* 2015].

In practical applications, supply water temperature and water flow rate are commonly used for the Radiant Heating and Cooling systems control. An outdoor temperature reset control is typically applied, which modulates the supply water temperature depending on the outdoor air temperature and controls water flow rate to each room according to the room set point temperature [Ryu *et al.* 2004]. It is also recommended that the

average water temperature (mean value of supply and return water temperature) be controlled according to the outside and/or indoor temperature because this can result in faster and more accurate control of the thermal output to the space. In certain cases, the slab or floor surface temperatures could be used as a controlled parameter in order to improve energy efficiency or to avoid local discomfort [Shin *et al.* 2015]. In a building with a radiant floor heating system, the improper installation of a sensor that measures the floor surface temperature can lead to under-heating or local over-heating conditions, especially when the floor covering and solar radiation significantly affect the temperature distribution in the floor surface [Athienitis 1997]. When the TABS is used as a primary heating system for comfort heating, the heating system should be wired in series with a slab-sensing thermostat, which acts as a limit switch to control the maximum surface temperatures (27-29 °C) [ISO 2005]. For the indoor temperature, it is preferable to control room temperature as a function of the operative temperature in order to achieve better thermal comfort. Gwerder et al. [Gwerder *et al.* 2008] suggested an intermittent operation with pulse width modulation (PWM) control, considering the prediction uncertainty of heat gains during operation, which proved to reduce the pumping energy by 50% more than the continuous pump operation [Lehmann *et al.* 2011].

3.3 Models of Radiant Heating Systems

There are a lot of ways to classify models developed of radiant systems. Despite the different adopted approaches, most such models aim to quantify the indoor thermal comfort, the energy consumption of the system and the thermal output of the system. Below are the commonly adopted modeling techniques of radiant heating systems in recent studies:

- Computational models of indoor air. In these models, finite element and finite volume methods are used to examine the thermal and flow distribution inside the conditioned space using CFD (Computational Fluid Dynamics) tools. Air inlets and outlets, radiative terminals, windows, doors, human bodies, appliances, and furniture are treated as mass or thermal boundary conditions. The temperature distribution in radiant slabs or panels is not solved. Instead, such surfaces are represented by specific mean surface temperatures. Mass, momentum, and energy conservation equations are solved in parallel with a radiation model of the space (typically surface-to-surface or discrete ordinates models). As for solar radiation, it can be defined as heat flux or solved in the simulation tool using ray-tracing methods, given the location and geometry of the building, and date and time of the simulation. Despite being the most accurate approach for examining the indoor environment, the simulation is typically carried out under steady-state conditions due to the intensive computational costs [Liu *et al.* 2020] [Kong *et al.* 2017].

- Computational models of radiant slabs or panels. In these models, numerical methods such as finite difference (FDM), element (FEM), or volume (FVM) are used to examine the temperature distribution in radiant bodies to determine their heating capacities. Here, the indoor air volume is represented as a boundary condition on the surface of the panel/slab. Usually, the performance of the panel/slab is characterized under steady-state conditions for specific mean water and surface

temperatures. The exact geometry of the body is often simplified by neglecting the end losses of the panel, the variation in water temperature, and the variations in the properties of the fluid and the panel/slab. These models are often reduced to 2-D ones [Chen and Li 2021] [González and Prieto 2021].

- Simplified analytical or numerical models of the conditioned space and the radioactive terminals. These simplified 0-D or 1-D models are meant to be used in transient simulation tools to examine the dynamics of the cooling systems throughout a typical heating day or throughout the whole heating season. The most popular analytical model is the R-C (resistor-capacitor) model suggested by Ren and Wright [Ma *et al.* 2013].

- Regression and data-driven models. These models are often developed as a part of adaptive and predictive control strategies. They are used to predict the heating loads of different zones of the building for determining a control strategy that minimizes the power consumption while maintaining the indoor environment in the comfort range [Koschwitz *et al.* 2018].

Intentionally blank page.

Chapter 4

Analytic Setup

The simulation and calculation of the underfloor heating system by doing a numerical analysis or using analytical equations can help to investigate the thermal behavior of the system, for different constructive solutions. This behavior depends on several parameters that characterize the underfloor heating system. Surface temperature and heat flux output of radiant floor are the key outputs for the design and control of radiant floor heating and cooling systems. The two outputs subject to analysis are the two mentioned before due to their importance.

A parametric study is carried out using a reference radiant floor system structure, with parameters previously defined. By successively changing the values of each parameter while maintaining the rest constant, it is possible to analyze the variation of the surface temperature and heat flux. In this way, it is possible to evaluate the parameters that should have more attention in the dimensioning of the underfloor heating system, and which values of these parameters provide a better performance of the underfloor heating system.

4.1 Pipe Spacing Influence

An article developed design charts to help designers consider heat flux, difference between maximum and minimum floor surface temperature (DFST), and maximum floor surface temperature (MFST) at the design stage through investigating the relationship between heat flux and design parameters [Shin *et al.* 2015]. This study covers a radiant floor heating panel with embedded pipes, Figure 4.1, which is the most common radiant floor panel system where this study was conducted, in this case Korea.

The variable of interest in this case is the spacing between the two pipes which is designated by M. The required average water temperature, t_{w}, for the specific heat flux q can be calculated using Equation 4.1.

$$t_{\mathrm{w}} = (q + q_{\mathrm{b}})\, M R_{\mathrm{t}} + t_{\mathrm{d}} \tag{4.1}$$

Where:
q is the total heat flux on floor panel surface [W/m^2]
q_{b} is the heat flux of back and perimeter heat losses in a heated panel [W/m^2]
M is the pipe spacing [m]
R_{t} is the thermal resistance between pipe wall per unit tube spacing in a hydronic system [(mK)/W]

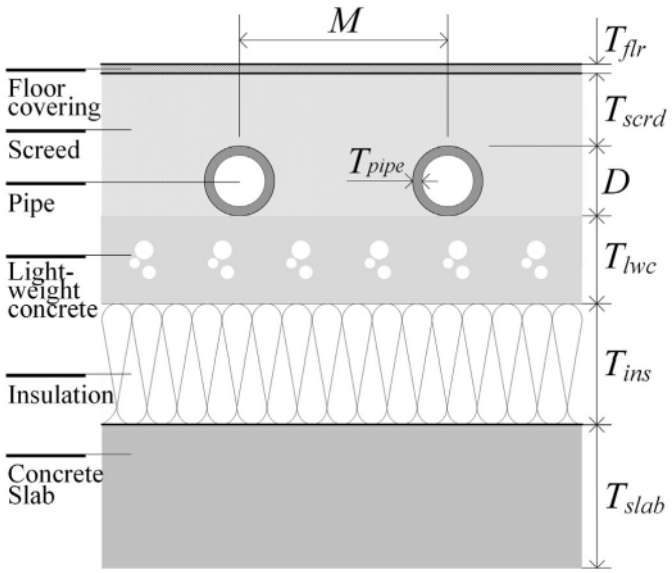

Figure 4.1: Section of the radiant floor heating panel with embedded pipes [Shin *et al.* 2015]

t_{d} is the average skin temperature of the pipe [°C]
t_{w} is the required average water temperature [°C]

To study the effects of pipe spacing, Equation 4.1 is solved for k and the values of the other variables will be assigned for the purpose of evaluating the influence of pipe spacing, considering the heat flux of back and perimeter heat losses, q_{b} as 10% of k. Solving the last equation for q, Equation 4.2 results.

$$q = \frac{t_{\mathrm{w}} - t_{\mathrm{d}}}{1.1\,(MR_{\mathrm{t}})} \tag{4.2}$$

The goal of this study is to maximize heat flux, which is a direct calculation using the previous equation because the only variable being studied is the pipe spacing. Heat flux is an important metric, given a specific room which requires a specific amount of heating flux, the right pipe spacing distance can be found at an early designing stage to fulfill those heating requirements. Table 4.1 presents the values of the constant variables. These values were taken from the paper in which this analytical equation was developed.

Table 4.1: Values of the constant variables for spacing research.

Variable	
Required average water temperature [°C]	35.00
Average skin temperature of the pipe [°C]	32.00
Thermal resistance between pipe wall per unit tube spacing [(mK)/W]	1.00

Using these values, heat flux was calculated using different values of spacing ranging from 40 mm to 400 mm. Figure 4.2 shows the results of the effect of tube spacing on heat flux.

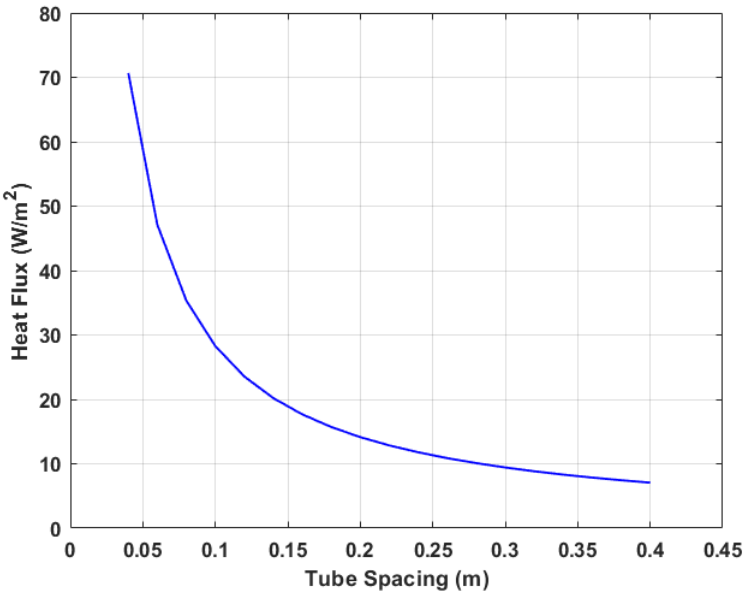

Figure 4.2: Effect of tube spacing on heat flux.

In the case of spacing, the lower spacing value the more heat flux is generated, there are also some constraints to take into consideration when choosing this value such as geometrical and dimensional constraints. With the increase of pipe spacing, floor surface temperature decreases significantly. It can also cause some discomfort because some areas of the flooring will be at a bigger temperature than other ones. Using more narrow spacing also requires a larger pipe length resulting in a higher construction cost.

4.2 Heat Transfer Between Heated Fluid and Piping

The effects of the tube and the fluid that runs through it can also be analysed, here the tubing will be looked at as an isolated component. Using Equation 4.3 the heat flux between the heated fluid and pipes, Q_{f}, can be evaluated.

$$Q_{\mathrm{f}} = \frac{T_{\mathrm{cu},0} - T_{\mathrm{w}}}{\frac{1}{\pi D_{\mathrm{i}} h_{\mathrm{f}}} + \frac{1}{2\pi k_{\mathrm{p}}} \ln \frac{D_{\mathrm{o}}}{D_{\mathrm{i}}}} \tag{4.3}$$

Where
$T_{\mathrm{cu},0}$ is the external surface temperate of the pipes [K]
T_{w} is the fluid temperature [K]
D_{i} is the internal diameter of the pipes [m]
D_{o} is the external diameter of the pipes [m]
h_{f} is the convection heat transfer coefficient of the internal flow [W/ $\left(\mathrm{m}^2\mathrm{K}\right)$]
k_{p} is the thermal conductivity of the pipes [W/ (mK)]

To calculate the convection heat transfer coefficient of the internal flow, Equation 4.4 will be used

$$h_{\mathrm{f}} = \frac{k_{\mathrm{w}} N u_{\mathrm{f}}}{D_{\mathrm{i}}} \tag{4.4}$$

Where
Nu_{f} is the local Nusselt number
K_{w} is the thermal conductivity of the fluid [W/ (mK)]

The local Nusselt number of turbulent flows in circular tubes can be obtained from Equation 4.5

$$Nu_{\mathrm{f}} = 0.023 {Re_{\mathrm{f}}}^{4/5} Pr_{\mathrm{f}}^{0.4} \tag{4.5}$$

Where
Re_{f} is the Reynolds number
Pr_{f} is the Prandtl number

The Reynolds number and Prandtl number are calculated using Equation 4.6 and Equation 4.7.

$$Re = \frac{\rho v L}{\mu} \tag{4.6}$$

$$\mathrm{Pr} = \frac{\mu C_{\mathrm{p}}}{k} \tag{4.7}$$

Where
ρ is the fluid density [kg/m^3]
v is the flow speed [m/s]
emphL is the characteristic linear dimension, in this case the internal diameter [m]
μ is the dynamic viscosity [Pa s]
C_{p} is the specific heat capacity [J/kg $\cdot$ °C]
k is the thermal conductivity [W/m.°C]
The values used to calculate the Reynolds and Prandtl number are present in Table 4.2 and Table 4.3.

Table 4.2: Properties of the fluids.

Fluid	ρ [kg/m^3]	μ [Pa s]	C_p [J/kg $\cdot$ °C]	k [W/m.°C]
Water	997.00	0.00089	4180.00	0,60
PG20	1030.00	0.002	3900.00	0.51
PG50	1080.00	0.0066	3300.00	0.40
PG60	1100.00	0.01	3100.00	0.38
PG80	1120.00	0.021	2800.00	0.34

With this, heat flux from the piping alone is calculated and the influence of the fluid evaluated. The external and internal diameter influence will also be calculated, the

difference between these two is the thickness of the tube itself which is also a parameter to take into account when choosing the tubing used. The final parameter evaluated is the material of the tubing which will be evaluated by changing its thermal conductivity. The first step of this study is calculating the Nusselt number using Equation 4.5 to then determine the convection heat transfer coefficient of the internal flow with Equation 4.4. The final stage is to calculate the value of the heat flux using Equation 4.3.

Table 4.3: Values of the constant variables for piping analysis.

Variable	
$T_{cu,0}$, Pipe external surface temperature [°C]	30.00
T_w, Fluid temperature [°C]	35.00
Fluid	Water
V, Flow speed [m/s]	0.60
D_i, Internal diameter [m]	0.018
D_o, External diameter [m]	0.020
k_p, Thermal conductivity of the pipe [W/m.°C]	0.21

With all the previous values, all the calculations are done. The first step is to find the best fluid to use taking into account Table 4.2 for the properties of the fluids available, these were chosen taking into account what is currently used in the market. Currently, the choice lies between water and water with propylene glycol solutions, when it comes to these water based solutions, the percentage of propylene glycol is the parameter that can vary. To choose the best fluid the values present in Table 4.3 are used, with these values heat flux will be calculated using Equation 4.3.

As it can be seen in Table 4.4, the best fluid to use is Water, the choice of the fluid may also have to take into account the anti freezing properties that glycol provides to the fluid. With Water as the chosen fluid all the different variables will be studied.

Table 4.4: Heat flux results for each fluid.

Fluid	Heat Flux [W/m^2]
Water	116.42
PG20	112.27
PG50	102.51
PG60	98.40
PG80	89.30

Figure 4.3 presents the influence of four different parameters on heat flux where it can be seen that by far the most important variable is the thermal conductivity of the pipe used.

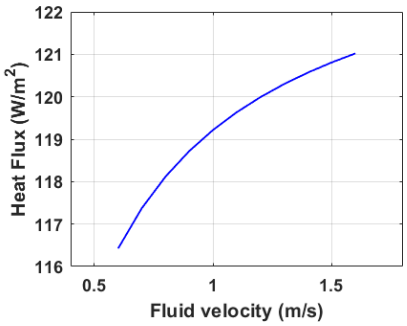

(a) Effect of fluid velocity (V) on heat flux.

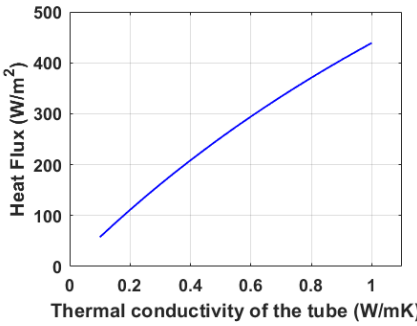

(b) Effect of thermal conductivity of the pipe (k_{p}) on heat flux.

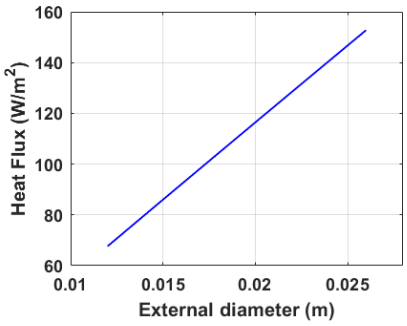

(c) Effect of pipe external diameter (D_o) on heat flux.

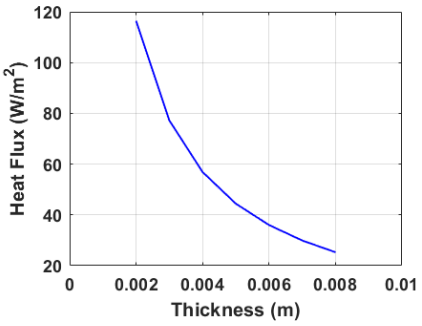

(d) Effect of pipe thickness ($D_o - D_i$) on heat flux.

Figure 4.3: Effect of different piping parameters on heat flux.

To get the optimal solution, Excel solver is used, resourcing three different optimization methods available, as described below [Barati 2013] [Hashemi *et al.* 2020]:

- GRG Nonlinear – GRG stands for "Generalized Reduced Gradient". In its most basic form, this solver method looks at the gradient or slope of the objective function as the input values (or decision variables) change and determines that it has reached an optimum solution when the partial derivatives equal zero. The downside is that the solution you obtain with this algorithm is highly dependent on the initial conditions and may not be the global optimum solution. The solver will most likely stop at the local optimum value nearest to the initial conditions, giving you a solution that may or may not be optimized globally.

- Simplex LP – Limited in its application because it can be applied to problems containing linear functions only, however, it is very robust, because if the problem trying to be solved is linear the solution obtained by the Simplex LP method is always a globally optimum solution.

- Evolutionary – The Evolutionary algorithm is more robust than GRG Nonlinear because it is more likely to find a globally optimum solution. However, this solver method is also slower when compared to the other two. The Evolutionary method is based on the Theory of Natural Selection. In simple terms, the solver starts with a random "population" of sets of input values. These sets of input values are put into the model and the results are evaluated relative to the target value. The sets of input values that result in a solution that is closest to the target value are selected to create a second population of "offspring". The offspring are a "mutation" of that best set of input values from the first population. The second population is then evaluated and a winner is chosen to create the third population. This goes on until there is very little change in the objective function from one population to the next. What makes this process so time-consuming is that each member of the population must be evaluated individually. Also, subsequent "generations" are populated randomly instead of using derivatives and the slope of the objective function to find the next best set of values.

After having the information about these algorithms GRG Nonlinear and Evolutionary are chosen to solve the optimization problem, the variables that are included in this are the material of the piping, the external and internal diameter of the tubing and the velocity of the fluid.
To get the optimal solution, constraints that make sense in the context of a radiant floor system were put in place for all those variables.
The formulation of the optimization problem is present in Equation 4.8 and the corresponding constraints in Equation 4.9.

$$\text{Maximize } Q_{\mathrm{f}}\left(D_0, D_{\mathrm{i}}, V, k_{\mathrm{p}}\right) = \frac{T_{\mathrm{cu}} - T_{\omega}}{\frac{1}{\pi D_{\mathrm{i}} \frac{k_{\omega} N_u}{D_{\mathrm{i}}}} + \frac{1}{2\pi k_{\mathrm{cu}}} \ln\left(\frac{D_0}{D_{\mathrm{i}}}\right)} \tag{4.8}$$

Subject to,

$$\begin{aligned} &0.012 \leq D_0 \leq 0.026 \text{ m} \\ &0.010 \leq D_\text{i} \leq 0.024 \text{ m} \\ &0.60 \leq V \leq 1.60 \text{ m/s} \\ &0.10 \leq k_\text{p} \leq 1.1 \text{ W/mK} \\ &D_0 - D_\text{i} = 0.0020 \text{ m} \end{aligned} \tag{4.9}$$

With those variables the same optimal result was achieved using both methods, the evolutionary algorithm took more time to reach the final solution than GRG Nonlinear. The values of the variables for the optimal solution are present in Table 4.5:

Table 4.5: Values of the optimal solution.

Variable	
Fluid	Water
V, Flow speed [m/s]	1.60
D_i, Internal diameter [m]	0.024
D_o, External diameter [m]	0.026
k_p, Thermal conductivity of the pipe [W/ (mK)]	1

With these values the calculated heat flux is $Q_\text{f} = 670.18\ W/m^2$

It can be concluded that the best possible result to maximize heat flux is to get the values of the variables to the upper or lower limit of it depending on the behaviour of the variable.

4.3 Analytic Radiant Floor System Evaluation

A study created a simplified calculation of the average surface temperature and the heat flux of a radiant floor system [Zhang *et al.* 2012], a scheme of the slab analysed is present in Figure 4.4.

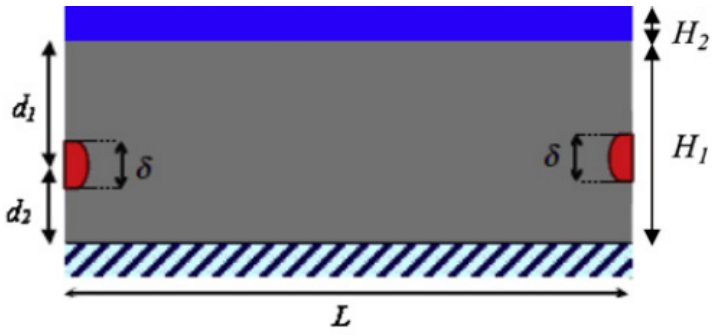

Figure 4.4: Section of the radiant floor heating panel with embedded pipes [Zhang *et al.* 2012].

For an actual radiant floor, which is composed of two layers and a water pipe, the heat resistance of each layer and heat resistance from the water pipe can be expressed,

where R_1 is the resistance of the layer where the piping is embedded calculated using Equation 4.10. R_2 is the resistance of the surface layer determined using Equation 4.13 and R_d is the resistance of the piping calculated using Equation 4.14:

$$R_1 = \frac{L}{2\pi k_1}\left[\ln\left(\frac{L}{\pi\delta}\right) + \frac{2\pi k_1}{L}\frac{d_1}{k_1} + \sum_{s=1}^{\infty}\frac{G(s)}{s}\right] \tag{4.10}$$

Where
L is the spacing between the pipes [m]
k_1 is the thermal conductivity of the piping layer [W/m.°C]
δ is the external diameter of the tubes [m]
d_1 is the distance between the piping and the upper edge of the piping layer [m]
G(s) is calculated using Equation 4.11

$$G(s) = \frac{\frac{Bi+2\pi s}{Bi-2\pi s}e^{-\frac{4\pi s}{L}d_2} - 2e^{-\frac{4\pi s}{L}(d_1+d_2)} - e^{-\frac{4\pi s}{L}d_1}}{\frac{Bi+2\pi s}{Bi-2\pi s} + e^{-\frac{4\pi s}{L}(d_1+d_2)}} \tag{4.11}$$

Where
Bi is Biot Number
d_2 is the distance between the piping and the lower edge of the piping layer [m]
Biot number is calculated using Equation 4.12

$$Bi = \frac{h_\mathrm{tot}L}{k_1} \tag{4.12}$$

Where
h_tot is the total heat transfer coefficient [W/ $\left(\mathrm{m}^2\ \mathrm{K}\right)$]

$$R_2 = \frac{H_2}{k_2} \tag{4.13}$$

Where
H_2 is the thickness of the surface layer [m]
k_2 is the thermal conductivity of the surface layer [W/m.°C]

$$R_\mathrm{d} = \frac{H_\mathrm{d}}{k_\mathrm{d}} \times \frac{L}{\pi\delta} \tag{4.14}$$

Where
H_d is the thickness of the pipes [m]
k_d is the thermal conductivity of the pipes [W/m.°C]

The heat resistance of the radiant floor itself from pipe to surface is:

$$R_\mathrm{S} = R_1 + R_2 + R_\mathrm{d} \tag{4.15}$$

The equation found to calculate the surface temperature is Equation 4.16

$$T_\mathrm{S} = \frac{T_\mathrm{m} + \left(R_\mathrm{op}h_\mathrm{tot} - 1\right)T_\mathrm{op}}{R_\mathrm{op}h_\mathrm{tot}} = \frac{T_\mathrm{m} + R_\mathrm{s}h_\mathrm{tot}T_\mathrm{op}}{R_\mathrm{s}h_\mathrm{tot} + 1} \tag{4.16}$$

Where
T_{m} is the mean temperature of supply and return water [°C]
T_{op} is the operative temperature [°C]

To calculate the total heat flux of the radiant floor Equation 4.17 is used.

$$q_{\mathrm{tot}} = \frac{T_{\mathrm{op}} - T_{\mathrm{m}}}{R_{\mathrm{op}}} = \frac{T_{\mathrm{S}} - T_{\mathrm{m}}}{R_{\mathrm{S}}} \tag{4.17}$$

To calculate the influence of each variable a study similar to the one before is done where variables will be constant and then one of them will change from a range that makes sense in the context of the problem, the values of these constant variables is present in Table 4.6.

Table 4.6: Values of the constant variables for radiant floor system analysis.

Variable	
L, Spacing between the Tubing [m]	0.100
k_1, Thermal Conductivity of the Piping Layer	0.50
δ. External Diameter of the Tubes [m]	0.02
d_1, Distance between the piping and the upper edge of the piping layer [m]	0.050
d_2, Distance between the piping and the lower edge of the piping layer [m]	0.050
h_{tot}, Total heat transfer coefficient [W/ $\left(\mathrm{m}^2\ \mathrm{K}\right)$]	11.00
H_2, Thickness of the Surface Layer [m]	0.006
k_2, Thermal Conductivity of the surface layer [W/m.°C]	0.10
H_d, Thickness of the Pipes [m]	0.002
k_d, Thermal Conductivity of the Pipes [W/m.°C]	0.10
T_m, Mean Temperature of Supply and Return Water [°C]	35
T_{op}, Operative Temperature [°C]	21

In Figure 4.5 and Figure 4.6 there are graphics showcasing the influence of multiple individual parameters on the heat flux of the radiant floor system. These parameters are: distance of the pipe in the vertical relative to the upper edge of the tubing layer; the thickness of the tubing layer; the thickness of the surface layer; the thickness of the tubes; the external diameter of the tubes; the thermal conductivity of the surface layer; the thermal conductivity of the tubing layer; the conductivity of the tubes; the spacing between the pipes.

Analysing all these graphics, the three most influential parameters are the distance of the tubes to the surface of the floor, the spacing between the tubes and the thickness

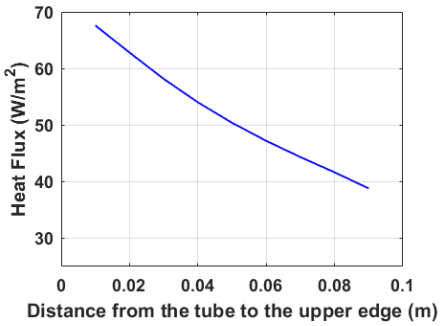

(a) Effect of distance of piping to the surface (d_1) on heat flux.

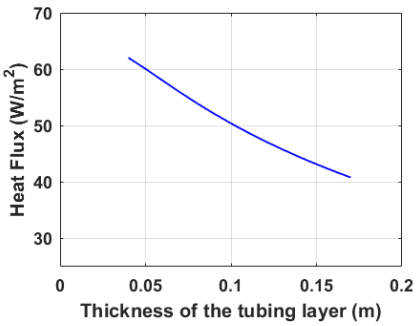

(b) Effect of tube layer thickness ($d_1 + d_2$) on heat flux.

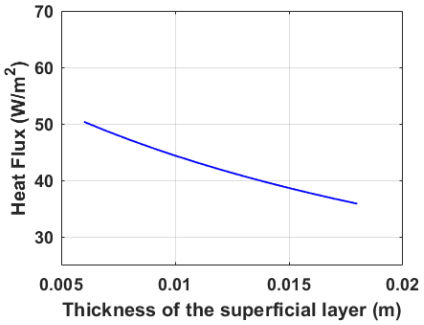

(c) Effect of surface layer thickness (H_2) on heat flux.

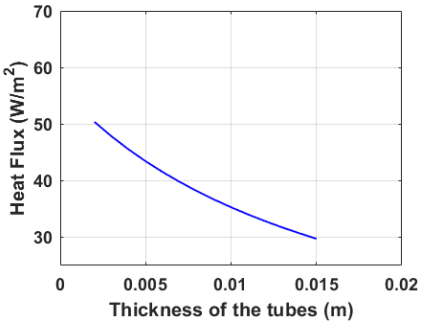

(d) Effect of pipe thickness (H_d) on heat flux.

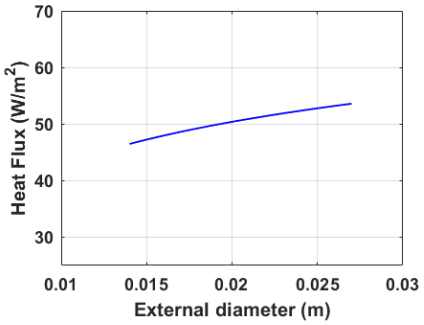

(e) Effect of pipe external diameter (δ) on heat flux.

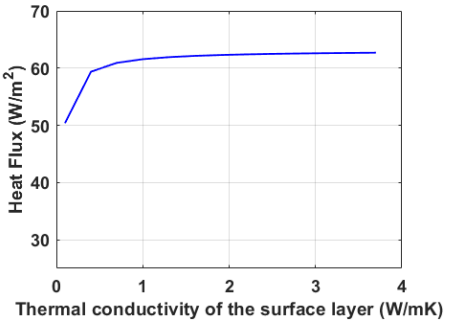

(f) Effect of surface layer conductivity (k_2) on heat flux.

Figure 4.5: Effect of different parameters on radiant floor heat flux.

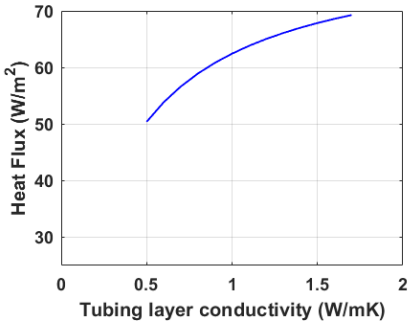

(a) Effect of tubing layer conductivity (k_1) on heat flux.

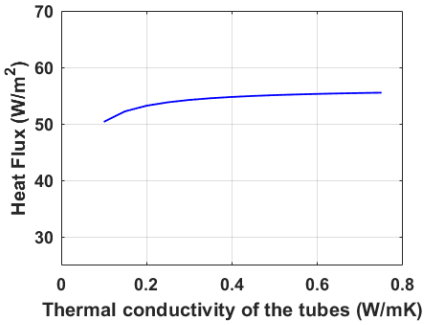

(b) Effect of tube conductivity (k_d) on heat flux.

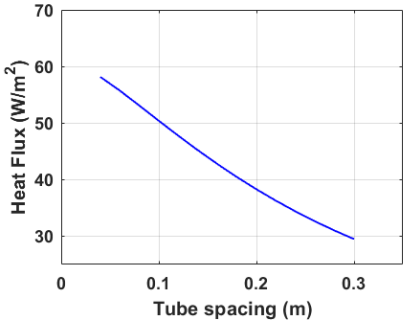

(c) Effect of tube spacing (L) on heat flux.

Figure 4.6: Effect of different parameters on radiant floor heat flux.

of the multiple layers. The least influential parameter is the thermal conductivity of the tube.

Using Excel solver to find the optimal solution, constraints were put in place for all those variables. These constraints were given to the variables listed before, with some of these constraints being put in place to not give impossible geometries. The values for these restrictions are put in place using the context of the problem in the real world. For example, a tube with a diameter of 100 millimeters does not make sense for a radiant floor system, etc.

The formulation of the optimization problem is present in Equation 4.18 and the corresponding constraints in Equation 4.19.

$$\text{Maximize } q_{\text{tot}}\left(L, k_1, \delta, d_1, d_2, k_2, H_2, k_{\text{d}}, H_{\text{d}}\right) = \frac{T_{\text{S}} - T_{\text{m}}}{R_{\text{S}}} \tag{4.18}$$

Subject to ,

$$
\begin{aligned}
&0.04 \leq L \leq 0.300 \text{ m} \\
&0.5 \leq k_1 \leq 1.7 \text{ W/m.°C} \\
&0.014 \leq \delta \leq 0.027 \text{ m} \\
&0.020 \leq d_1 \leq 0.170 \text{ m} \\
&0.020 \leq d_2 \leq 0.170 \text{ m} \\
&0.1 \leq k_2 \leq 3.7 \text{ W/m.°C} \\
&0.006 \leq H_2 \leq 0.018 \text{ m} \\
&0.1 \leq k_d \leq 0.75 \text{ W/m.°C} \\
&0.002 \leq H_d \leq 0.015 \text{ m} \\
&\frac{\delta}{2} \leq L \\
&\frac{\delta}{2} \leq d_1 \leq (d_1 + d_2) - \frac{\delta}{2} \\
&\frac{\delta}{2} \leq d_2 \leq (d_1 + d_2) - \frac{\delta}{2} \\
&T_{\mathrm{S}} \leq 29 \text{ °C}
\end{aligned}
\tag{4.19}
$$

With those variables the same optimal result was achieved using both methods, the optimal solution is present in Table 4.7.

Table 4.7: Values of the optimal solution for a radiant floor system.

Variable	
L, Spacing between the Tubing [m]	0.04
k_1, Thermal Conductivity of the Piping Layer [W/m.°C]	0.87
δ. External Diameter of the Tubes [m]	0.027
d_1, Distance between the piping and the upper edge of the piping layer [m]	0.020
d_2, Distance between the piping and the lower edge of the piping layer [m]	0.050
H_2, Thickness of the Surface Layer [m]	0.006
k_2, Thermal Conductivity of the surface layer [W/m.°C]	0.18
H_d, Thickness of the Pipes [m]	0.002
k_d, Thermal Conductivity of the Pipes [W/m.°C]	0.10

With these values the calculated heat flux is $Q_{\mathrm{f}} = 99.00$ W/m^2 with a Surface Average temperature of $T_S = 29$ °C, this temperature is chosen as a limit due to previous research where it was found that it is the maximum temperature that does not cause discomfort.

Intentionally blank page.

Chapter 5

Numerical Setup

In this section, a numerical analysis is done to optimize a model of a radiant floor system. To perform this numerical simulation of a radiant floor system, a commercial simulation software called Ansys will be used. It offers a comprehensive suite of simulation solvers that spans a range of physics, providing access to virtually any field of engineering simulation that a design process requires. Ansys handles geometry, mesh, and Design Exploration process. The latter is used to solve the different Design of Experiments, create the response surfaces of outputs, and finally find points that optimize the geometries. The Ansys software was selected on the basis of its preciseness in terms of simulating mechanical properties, temperature distributions, heat transfer, and deformation [Meyghani *et al.* 2017].

5.1 Ansys Optimization Process

Design Exploration is a process used to investigate and evolve the design space intending to discover the optimal design and helping when it comes to decision making throughout the design process. The main purpose of Design Exploration is to identify the relation between the performance of the product and the design variables. Based on the results, the key parameters of the design can be identified and how they affect product performance. With this knowledge, it is possible to influence the design so it meets the product requirements. The parameterized model of the radiant floor system is built and the variable parameters that need to be optimized are settled in the Geometry module of ANSYS Workbench. The numerical simulation results which need to be optimized are set as the objective, after setting the optimization goal and the ranges of the variables, the optimal solution will be calculated.

The tool DesignXplorer includes several algorithms that help to identify the most suitable candidates, taking into account multiple objectives and performance trade-offs. DesignXplorer offers two types of optimization procedures, the Response Surface Optimization and Direct Optimization. With Direct Optimization there is no need to calculate the response surfaces or DOEs and the process can be started just by having the sampling space. The Response Surface Optimization (RSO) is based on a DOE and draws its information from the RS, hence it depends on the RS quality- [Menon 2005]. The computational time of this optimization is almost costless, the time is spent in the DOE step, after the DOEs are simulated and response surfaces are created, the next step

is analyzing the results with a correlation analysis using curves, surfaces, and sensitivities for example. After exploring the design and understanding correlations and sensitivities, the following step is to optimize the design to meet the required constraints. Optimal results are approximated since the algorithms use RS evaluation rather than solution from new simulations. On the other hand, Direct Optimization (DO) works with real solutions (new simulations), which means it has to run a new numerical simulation with new parameters, instead of using evaluations of the RS. As a result, changing the optimization criteria and rerunning is highly computationally time-consuming. Here, the optimal results rely on actual resolution. This optimization is suitable for cases where the computational time of each case is small and there is no interest in controlling the spatial distribution of design points or response surfaces.

Summing up, numerical simulation along with the DE allows to perform the best possible study of the case proposed. Simulation is necessary to reproduce the behavior of cases as if they were in a laboratory but in a cheaper way, the design of experiments is used to explore the sampling space in an efficient and effective mode.

5.1.1 Desing of Experiments (DOE)

DOE is a technique used to guide the choice of experiments to be performed efficiently. Within optimization procedure, an experiment is a series of tests in which the input variables are changed according to a rule to identify the reasons for the changes in the output response. There is a wide range of DOE algorithms or methods available in engineering literature. However, they all have common characteristics. They try to locate sampling points such that the space of random input parameters is explored in the most efficient way, or they try to get the required information with a minimum of points. Sample points in efficient locations not only reduce the required number of design points but also increase the accuracy of the response surface.

To perform a DOE, it is necessary to define the problem and choose the variables, which are called the factors or parameters. A design space or sampling space must be defined, i.e., a range of variability must be set for each variable. The number of values that the variables can assume in DOE is restricted and small. The DOE technique and the number of levels have to be selected according to the number of experiments which can be afforded. By the term levels it means the number of different values in which a parameter is discretized, that is usually the same for all. In the sampling space are placed the Design Points (DP), or sampling points, which represent every single simulation to be run.

5.1.2 Response Surface

Response Surfaces (RS) are functions in which the output parameters are described in terms of the input parameters. The main idea is to use the results of a DOE to create an approximation of the response variable over the design space. The reason for building a RS is that, although it is just an approximation, it can estimate the set of input parameters yielding an optimal response. The RS is an analytical function, thus the optimization process is quick and does not require additional experiments or simulations to be performed. From a mathematical point of view, the objective function, or response variable, r, is an unknown function of the input parameters p_i. The response surface $\widehat{r}$ is an approximation of this function and it is expressed as follows:

$$r = f(p_i) = \widehat{f}(p_i) + \epsilon(p_i) \quad \Longrightarrow \quad \widehat{r} = \widehat{f}(p_i), \tag{5.1}$$

where $\epsilon(p_i)$ is the estimation error.

The results of a DOE made of N simulations or experiments consists of $N(p_{ij}, r_j)$ couples in which a point p_{ij} of the design space is associated with the response value r_j. If $r_j = \widehat{f}(p_{ij})$ holds for each sample point, the RS is said to be an interpolating response, or an approximating response if the estimating error is not zero, $\epsilon(p_i) \neq 0$ [Khuri and Mukhopadhyay 2010].

5.1.3 Optimization of Design Points

Design points are generated according to the objectives and constraints of the system, depending on the user's settings. Out of the generated design points and for which the output parameter values were calculated, there are three points presented by the software that have the optimal output parameter values, these points being candidate points. Among the candidate points, the user chooses the optimal option to continue the project. The design point data, which has become the current point of the project, is inserted into the project input data, these being the key features on which the optimized project was created. The algorithm verifies the design points by creating and updating the output parameters with a real solution using the input points of the design points.

5.2 Ansys Optimization Algorithms

ANSYS provides a list of optimization algorithms [Exploration 2013, Grebenişan and Salem 2017, Somassoundirame and Nithiyananthan 2021]:

- **Screening**: Randomly sampling the space and pick out the good solutions, it is a direct sampling method that uses a quasi-random number generator based on the Hammersley algorithm [Salem 2017]. It is meant to be used as an initial trial to make sure everything is setup correctly, e.g., do the simulation results make sense in the context of the problem. Screening is typically used to find a first set of candidate points for a preliminary design. Then, if a refinement is required, these points are used as starting points for other optimization methods.

- **Multiobjective Genetic Algorithm (MOGA)**: Simultaneously find Pareto-optimal designs. MOGA can be used for both Response Surface Optimization and Direct Optimization. It is available for many types of input parameters and uses a genetic algorithm to generate the initial samples. Then, using cross-over and mutation for the next populations, it iteratively searches for the feasible points for creating the Pareto front.

- **Nonlinear Programming by Quadratic Lagrangian (NLPQL)**: Fast local search. Use this when there is only one objective, the simulation does not take too long, the number of variables is small, it is a gradient-based optimization methods for constrained problems and is based on quasi-Newton methods.

- **Mixed-Integer Sequential Quadratic Programming (MISQP)**: Similar to NLPQL in the sense that it is a gradient-based optimization methods for constrained problems too, but allows integer variables, it solves mixed-integer nonlinear programming by a modified sequential quadratic programming method.

- **Adaptive Single-Objective Optimization (ASO)**: This method uses Optimal Space Filling for DOE, Kriging as a response surface, and MISQP for finding local optimal solutions from the response surface. Use this when the evaluation of objective/constriants are expensive and there is a limited budget/time for optimization.

- **Adaptive Multi-Objective Optimization (AMO)**: Similar to ASO, this one uses Kriging and MOGA.

The choice of the optimization method depends on the properties of each case. In this project, a single-objective optimization method is needed. In Table 5.1 some optimization methods are shown and in which cases each one can be applied.

Table 5.1: Capabilities of the response surface optimization methods available in Ansys software [Exploration 2013].

Algorithm	Single objective	Multi objective	Local search	Global search	Discrete values
NLPQL	Yes	No	Yes	No	No
MISQP	Yes	No	Yes	No	Yes
Screening	No	Yes	No	Yes	Yes
MOGA	No	Yes	No	Yes	Yes

5.3 Radiant Floor System Setup

Previous chapters of this dissertation describe the theoretical concepts involved in the process of optimizing the radiant floor geometry to achieve maximization requirements. In this chapter, the case and setup details are presented. In the first part, the configuration of the case will be exposed, describing the geometry, the boundary conditions and the mesh. And in the last part, the optimization process is presented, reaching at the end the optimized solution and the conclusions drawn from this process.

The standard EN 1264 is a technical standard for designing and installing radiant floors for heating purposes. In the last years a revision of the standard took place in order to extend the existing calculation method for determining heat flow output also to other radiant systems (walls and ceilings) and operating conditions (heating and cooling). The standard presents the principles of a computer software verification in the direction of its suitability assessment for calculating the operating parameters of surface heating systems. The two parameters that are going to be analysed are the average surface temperature on the floor heating and the average heat flux released from its upper surface.

The calculations were performed for the floor heating system type A, which parameters are characterised by the standard EN 1264, an image of this type of system can be seen in Figure 5.1.

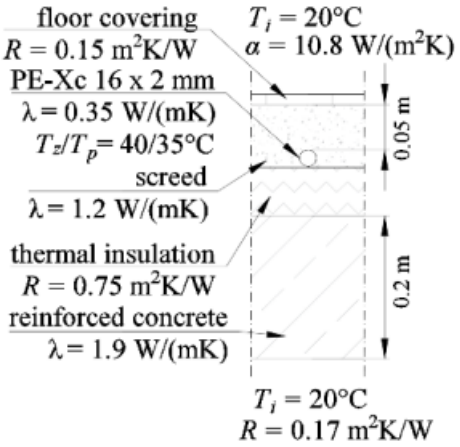

Figure 5.1: Model of a floor heating according to the EN 1264 standard [Exploration 2013].

The basic process of ANSYS Workbench simulation analysis can be divided into three parts: pre-processing where the geometric model is established, the material properties are defined and the mesh is created; solution where loads and constraints are defined and the solution is reached; and post-processing where you can view the analysis results and examine them.

The parameterized analysis has as its main objective the discovery and accentuation of the role of each input parameter on the evolution of the process, mainly on the output parameters chosen by the operator.

5.3.1 Mesh Independence Test

The mesh independence test is essential to ensure the simulation results are not affected by the mesh size. It shows us the limit till which we must refine our mesh to get accurate results, since further refining the mesh would only increase computation time. The mesh element size is the variable going to be changed ranging from 0.6 mm to 4 mm and consequently the corresponding number of elements is changing too. The two parameters that are going to be analysed are the average temperature of the body and the average heat flux.

Based on the grid independence test for the model shown in Figure 5.2 and Figure 5.3, the mesh element size of 1 mm or less is not affecting the results. Hence the mesh element size of 1 mm is the chosen one due to the lower computational time compared to the others.

Mesh refinement is an important tool for editing finite element meshes in order to increase the accuracy of the solution. The refinement is performed in an iterative procedure in which a solution is found, error estimates are calculated, and elements in regions of high error are refined. The circles need a refinement due to some of the mesh elements being triangles instead of the desired quadrilateral elements, this refinement

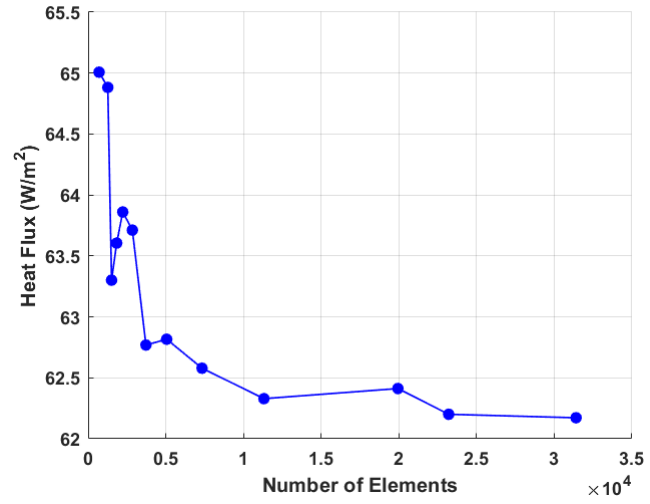

Figure 5.2: Convergence of Heat Flux results.

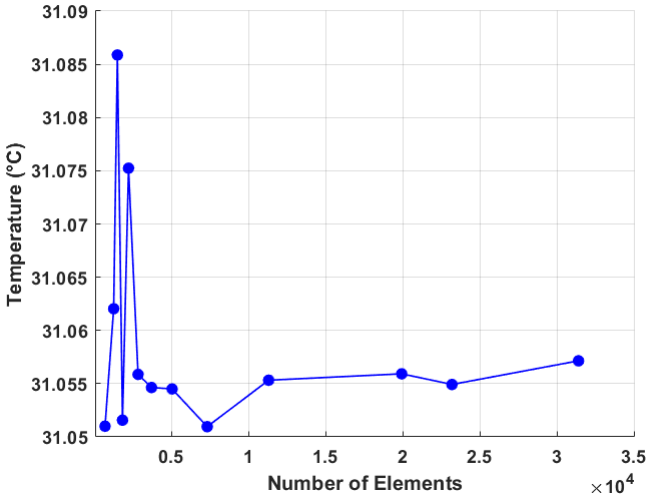

Figure 5.3: Convergence of Temperature results.

was done using Ansys resources of mesh refinement, the non refined mesh can be seen in Figure 5.4, after refining the mesh the end result is present in Figure 5.5 with all elements being quadrilateral.

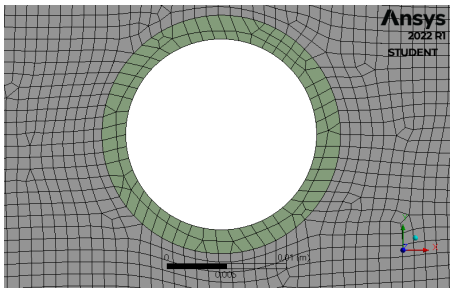

Figure 5.4: Mesh of the circle with no refinement.

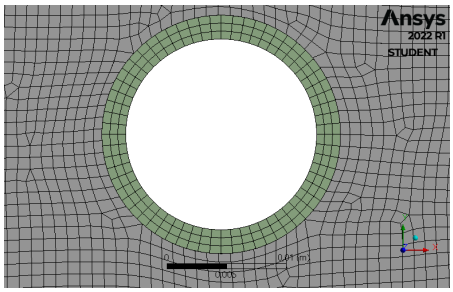

Figure 5.5: Mesh of the circle with refinement.

5.3.2 Model Validation

Using the definitions and boundary conditions of the previous model, the results of the numerical simulation were analysed and validated

In order to compare the results of calculations obtained with Ansys Software with the parameters obtained by the standard, the relative error of the heat flux density ε_{q} and the absolute error of the temperature ΔT were calculated from the following formulas:

$$\varepsilon_{\mathrm{q}} = \frac{|q_{\mathrm{Ansys}} - q_{\mathrm{v}}|}{q_{\mathrm{v}}} \cdot 100\% \tag{5.2}$$

$$\Delta T = |T_{\mathrm{Ansys}} - T_{\mathrm{v}}| \tag{5.3}$$

Where
q_{Ansys} is heat flux determined using Ansys [W/m^2]
q_{v} is heat flux calculated by EN1264 [W/m^2]
T_{Ansys} is the temperature determined using Ansys [°C]
T_{v} is the temperature calculated by EN1264 [°C]

The results of the simulations compared to the standard can be seen in Table 5.2, where W is pipe spacing.

The maximum difference between the average surface temperature of a floor heating T calculated using the ANSYS and standard EN 1264 was 0.73 °C for a pipe spacing of 0.45 m. The maximum difference between the heat flux released from the top surface of the floor heating q was 8.40 W/m^2 for a pipe spacing of 0.45 m. There are many factors that can be attributed for these differences such as a simplification of numerical model or mesh characteristics in ANSYS Meshing but an absolute error of less than 10% is acceptable.

5.3.3 Model Setup

The next step in the optimization process is modeling the system to be optimized. Using Design Modeler to build the geometry, the final model can be seen in Figure 5.6.

Table 5.2: Comparison of operating parameters of a floor heating system calculated according to EN 1264 and numerically with Ansys software.

W	Number of	q [W/m^2]		T [°C]		ε_q	ΔT
[m]	elements	EN 1264	Ansys	EN 1264	Ansys	[%]	[°C]
0.05	10219	57.94	58.70	25.36	25.87	1,30	0.51
0.10	11482	53.01	52.37	24.91	24.84	1,21	0.07
0.30	16474	37.36	39.17	23.46	22.94	4,84	0.52
0.45	20226	27.87	30.21	22.58	21.85	8,40	0.73

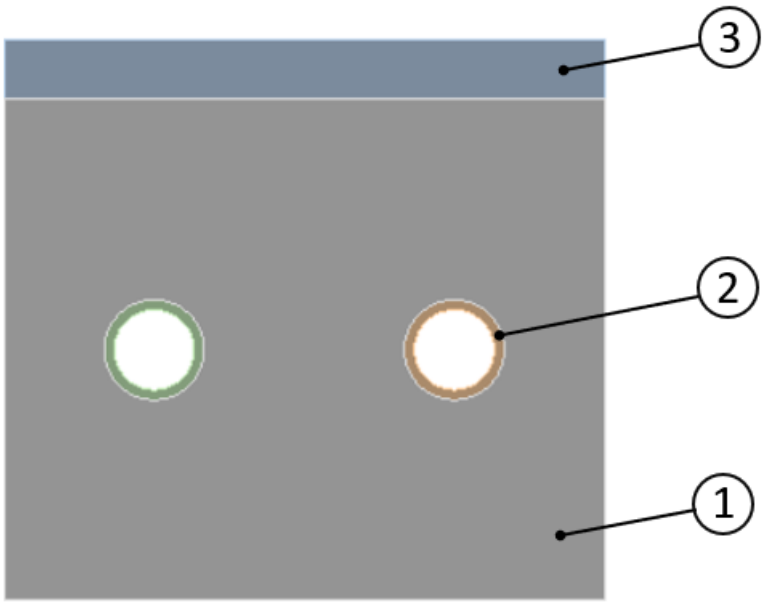

Figure 5.6: Radiant Floor System 2D model.

The materials used in this system were three. Concrete (1) is used for the layer where the tubes (2) are embedded. The material of these tubes is polyethylene and the surface layer material is oak (3). The materials used are inside a library of materials present on Ansys Software and their most important properties for thermal analysis are present in Table 5.3.

Where
ρ is the density of the material
CTE is the Coefficient of Thermal Expansion
k is the thermal conductivity
c_{p} is Specific Heat at constant pressure

Table 5.3: Properties of the materials.

Material	ρ [kg/m^3]	CTE [1/°C]	k [W/m.°C]	c_{p} [J/kg · °C]
Concrete	2392.00	1.02e-05	2.93	936.30
Polyethylene	950.00	2.30e-04	0.28	2300.00
Oak	935.70	4.69e-06	0.45	1685.00

After defining the materials of each layer the next step is to mesh the model using elements sized 1mm as previously defined. At this stage with the model already meshed, Figure 5.7, the previous validated boundary conditions are applied to the geometry of the model.

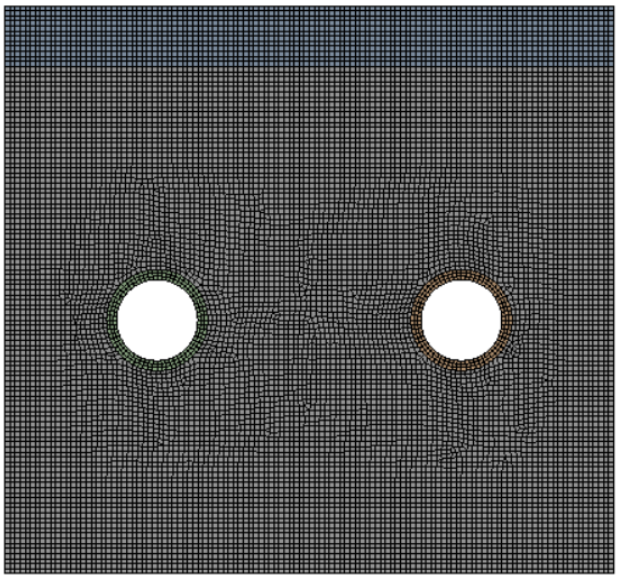

Figure 5.7: Radiant Floor System 2D meshed model.

After applying the boundary conditions, the numerical simulation is performed where the analysed outputs are the temperature and heat distributions throughout the 2D body.

The outputs analysed were the heat flux and average temperature at the surface. These values were measured resourcing to probes defined in the surface of the model.

Figure 5.8 and Figure 5.9 show the temperature and heat flux distributions of the system respectively, where it can be seen that along the surface of the system the temperature and heat flux is uniform.

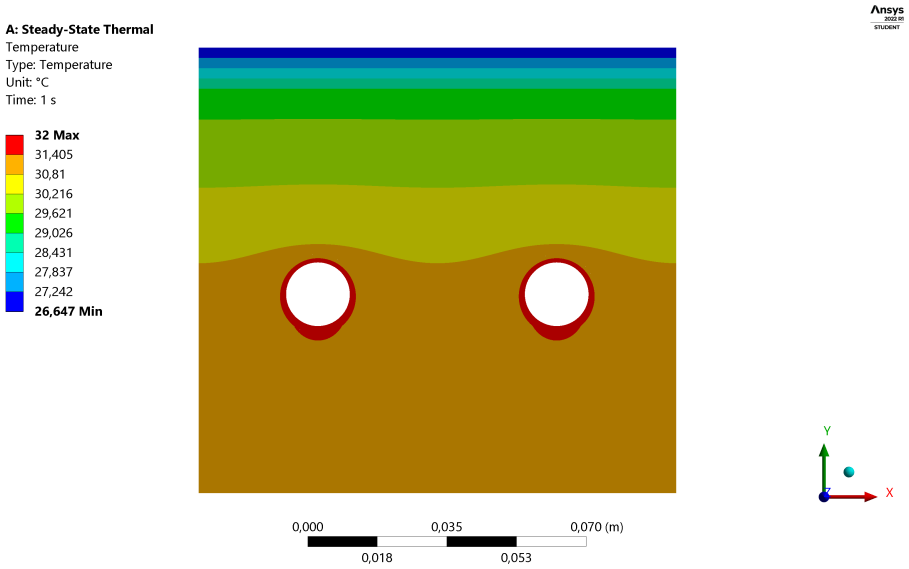

Figure 5.8: Temperature Distribution of the Radiant floor system.

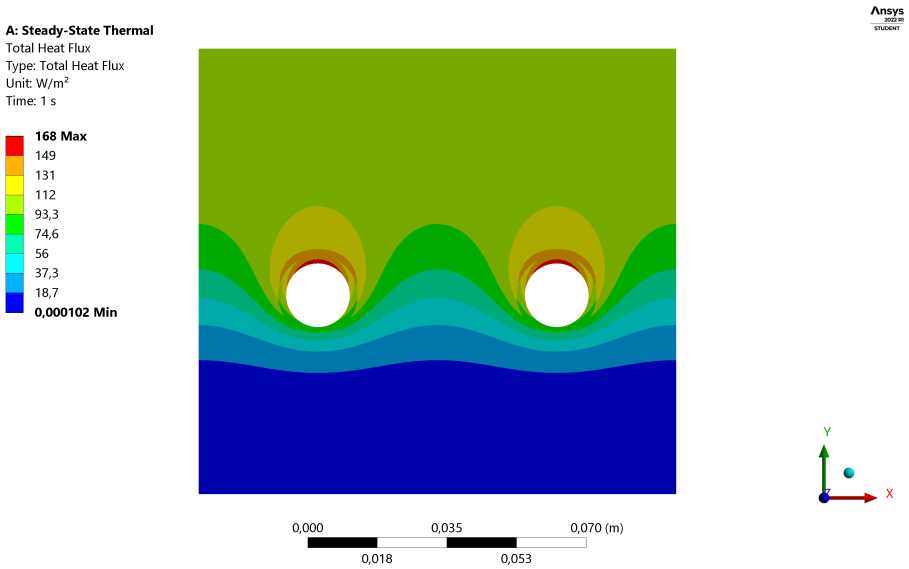

Figure 5.9: Heat Flux Distribution of the Radiant floor system.

5.3.4 Custom DOE

To get the local sensitivities of the variables it is necessary to perform a DOE. In this section, it is first presented the sensitivity analysis of the output parameters to see their global behavior regarding the input parameters. Then, the response surface of the most-affecting variables is studied, and finally, the optimization is performed to determine the design points which maximize heat flux.

Figure 5.10 shows the naming and measurements of the input parameters which are going to be analysed.

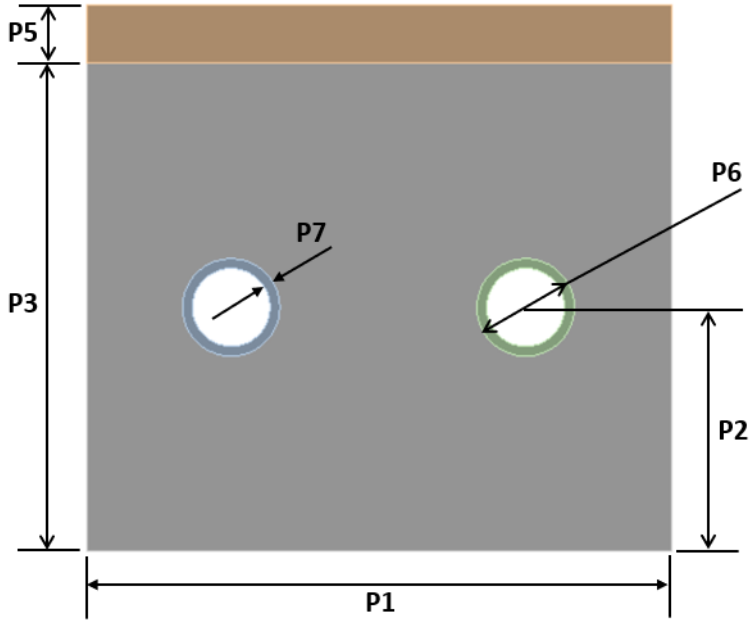

Figure 5.10: Measurements of the radiant floor slab.

5.3.5 Local Sensitivities

Local sensitivity charts are used to display the change of the output based on the variation of each input independently. A positive value of the sensitivity means that as the input parameter increases the output increases as well, and a negative value means the opposite.

Figure 5.11 shows the sensitivities analysis of the main output parameters, namely, i) the spacing between the tubing, ii) height of the tubing, iii) thickness of the tubing layer, iv) thickness of the tube, v) thickness of the surface layer and, vi) the external diameter.

One of the important aspects that can be appreciated in Table 5.4 and Table 5.5 is that the behavior of the input variables is exactly the same, with the same sensitivity values for their respective outputs.

Analysing the values provided by the sensitivity charts, Figure 5.11 and decreasing the values of the spacing between the tubing, the thickness of the tubing layer, the thickness of the surface layer, and thickness of the tubing, increases the heat flux and maximum surface temperature.

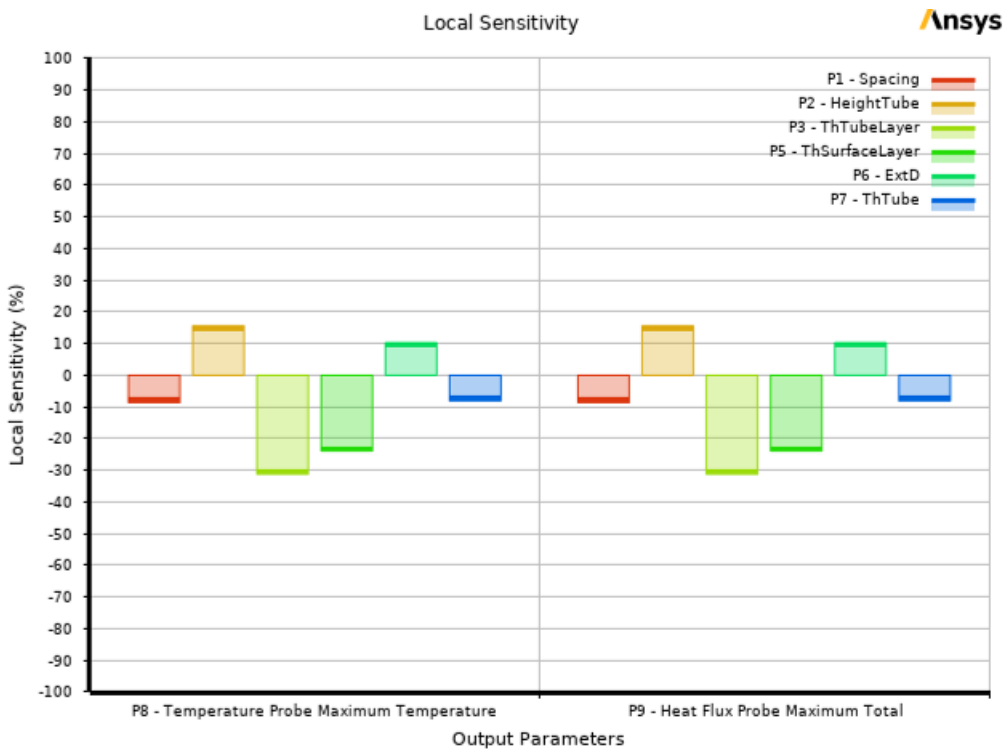

Figure 5.11: Sensitivities of the output parameters.

Taking into account the height of the tubing and the external diameter of the tubing, by increasing the values of these inputs, both outputs increase.

The most influential parameter, the one with the highest sensitivity value, is the thickness of the tubing layer followed by the thickness of the surface layer. This means that by changing the values of these two parameters the value of the outputs will consequently change.

Table 5.4: Values of the local sensitivities for the temperature probe maximum temperature.

P8, Surface Maximum Temperature	%
P1, Spacing between the tubing [m]	−8.67
P2, Height of the tubing [m]	15.58
P3. Thickness of the tubing layer [m]	−31.19
P5, Thickness of the surface layer [m]	−23.91
P6, External Diameter [m]	10.29
P7, Thickness of the tube [m]	−8.10

Table 5.5: Values of the local sensitivities for the maximum heat flux.

P9, Surface Maximum Heat Flux	%
P1, Spacing between the tubing [m]	−8.67
P2, Height of the tubing [m]	15.58
P3. Thickness of the tubing layer [m]	−31.19
P5, Thickness of the surface layer [m]	−23.91
P6, External Diameter [m]	10.29
P7, Thickness of the tube [m]	−8.10

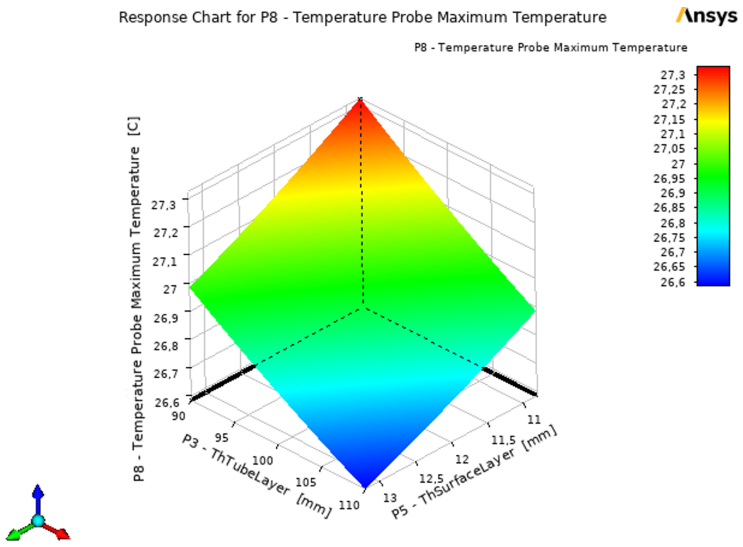

Figure 5.12: 3D Response surface of the Temperature Probe Maximum Temperature.

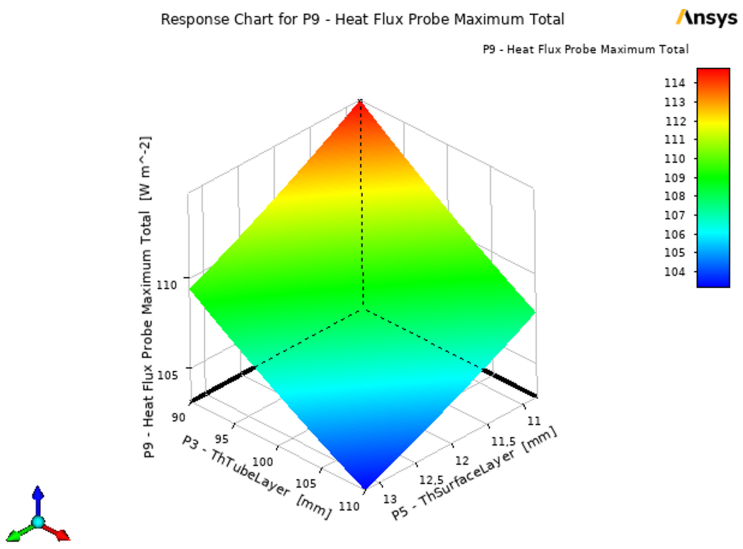

Figure 5.13: 3D Response surface of Heat Flux Probe Maximum Total.

Ansys provides 3D response surfaces to further analyse in the same graphic the influence of two input parameters on the output parameter.

Figure 5.12 and Figure 5.13 shows the influence of the two most important input parameters, the thickness of the tubing layer and the thickness of the surface layer on the surface temperature and heat flux respectively. It can be concluded that lower thickness results in higher temperature and heat flux.

Ansys also provides 2D graphics to check the influence of a single parameter on the output. Figure 5.14 and Figure 5.15 show the variation of the surface temperature and heat flux respectively, with respect to the thickness of the surface layer for different values of thickness of the tubing layer can be visualized.

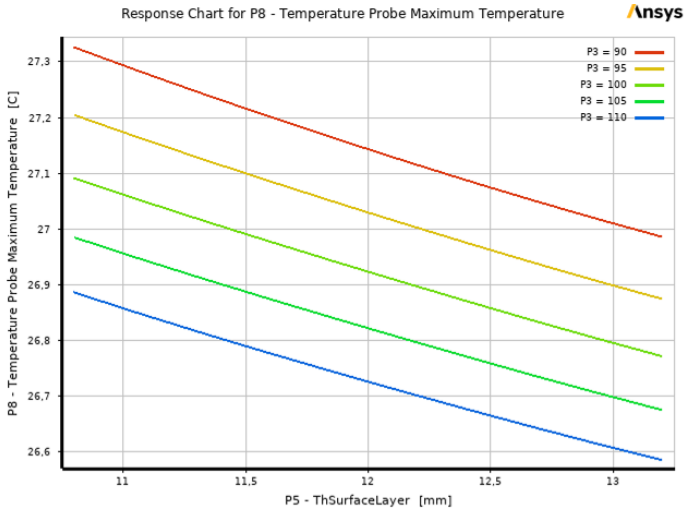

Figure 5.14: Variation of the surface temperature with respect to the thickness of the surface layer for different values of the thickness of the tubing layer.

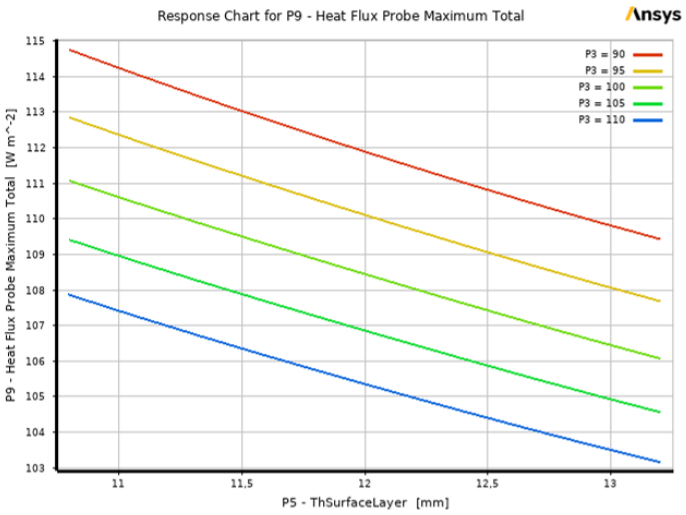

Figure 5.15: Variation of the surface heat flux with respect to the thickness of the surface layer for different values of the thickness of the tubing layer.

In Figure 5.16 and Figure 5.17 the variation of the surface temperature and heat flux respectively with respect to the thickness of the tubing layer for different values of the thickness of the surface layer can be visualized. The behavior of all the curves is the same when it comes to both outputs, justified by the fact that the values of the sensitivities are also equal. Compared to the analytic analysis done in the previous section, the behaviour of these curves is to be expected. With these curves the value of the outputs can be predicted and ultimately calculated.

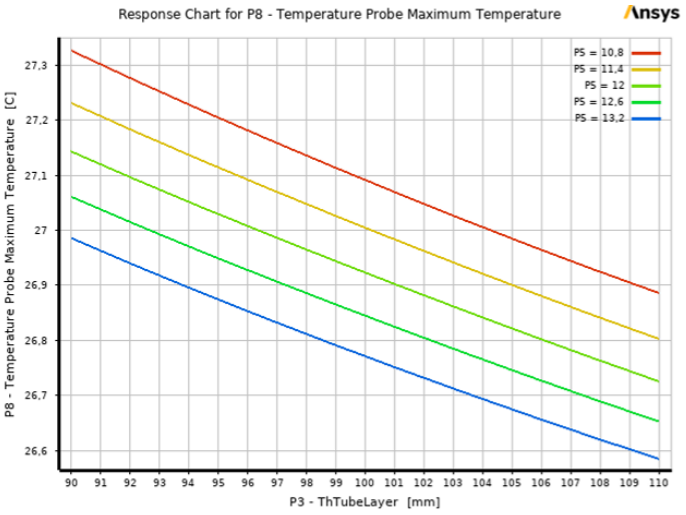

Figure 5.16: Variation of the surface temperature with respect to the thickness of the tubing layer for different values of the thickness of the surface layer.

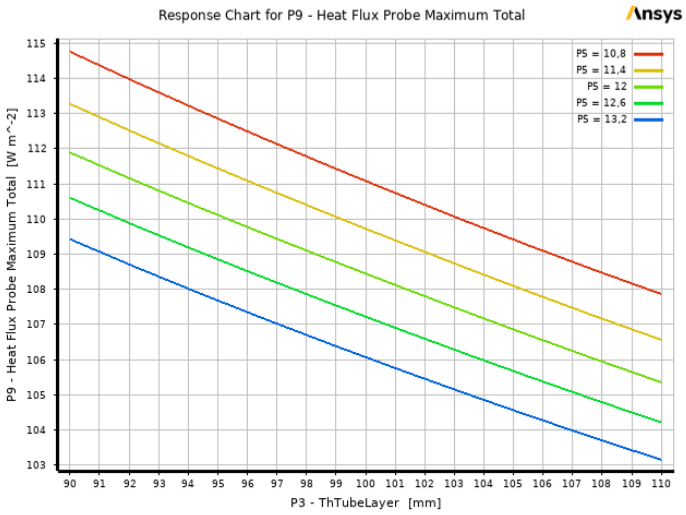

Figure 5.17: Variation of the heat flux with respect to the thickness of the tubing layer for different values of the thickness of the surface layer.

5.4 Optimization

Three different optimization algorithms have been used to perform the direct optimization: Adaptative single-objective, NLPQL, and MISQP are the algorithms used because of the fact that this optimization problem is a single objective one where the aim is to maximize surface heat flux with floor configurations that meet physical and geometrical constraints. Due to previous research the maximum surface temperature that is comfortable for a radiant floor system is 29°C, this value is set as an upper bound for the output of temperature probe maximum temperature.

5.4.1 Adaptative Single-Objective

This algorithm is configured to find 3 candidates in a maximum of 106 evaluations and 20 domain reductions, the solutions converged after 36 evaluations. Some of the points failed to simulate due to impossibilities in the geometries given some parameter values. Three candidate points were found and presented in Table 5.6:

This algorithm is the fastest of the three mentioned before, candidate point 1 provides the most surface heat flux out of all the candidate points with its geometrical dimensions.

Table 5.6: Candidate points proposed by Ansys software using ASO.

	Starting Point	CP 1	CP 2	CP 3
P1-Spacing (mm)	120.00	114.70	98.67	104.00
P2-HeightTube (mm)	50.00	45.00	63.00	79.00
P3-ThTubeLayer (mm)	100.00	82.00	90.00	96.67
P5-ThSurfaceLayer (mm)	12.00	8.27	9.33	12.27
P6-ExtD (mm)	20.00	20.93	16.13	21.20
P7-ThTube (mm)	2.00	1.15	1.35	1.25
P8-Surface temperature (°C)	26.93	28.14	28.08	28.04
Variation from reference (%)	0.00	4.49	4.27	4.12
P9-Surface heat flux (W/m^2)	108.50	128.20	127.40	126.80
Variation from reference (%)	0.00	18.16	17,42	16.87

5.4.2 NLPQL

This algorithm is gradiant based and the starting points must be specified to determine the region of the design space to explore. The configurations is done to approximate derivatives by forward difference and find 3 candidates in a maximum of 20 iterations.

The solutions converged after 83 evaluations. Three candidate points were found, which are presented in Table 5.7:

Table 5.7: Candidate points proposed by Ansys software using NLPQL.

	Starting Point	CP 1	CP 2	CP3
P1-Spacing (mm)	120.00	102.1	109.90	112.10
P2-HeightTube (mm)	50.00	72.18	63.24	60.75
P3-ThTubeLayer (mm)	100.00	85.75	91.46	93.04
P5-ThSurfaceLayer (mm)	12.00	8.30	9.78	10.19
P6-ExtD (mm)	20.00	20.92	20.55	20.45
P7-ThTube (mm)	2.00	1.305	1.57	1.65
P8-Surface temperature (°C)	26.93	29.00	28.02	27.78
Variation from reference (%)	0.00	7.70	4.05	3.18
P9-Surface heat flux (W/m^2)	108.50	142.10	126.30	122.6
Variation from reference (%)	0.00	30.94	16.44	13.00

5.4.3 MISQP

Mixed-Integer Sequential Quadratic Programming (MISQP) is similar to NLPQL because it is also a gradient based optimization method. The configurations is done to approximate derivatives by forward difference and find 3 candidates in a maximum of

20 iterations, the starting points must also be specified to determine the region of the design space to explore.

The solutions converged after 72 evaluations. Three candidate points were found, which are presented in Table 5.8:

Table 5.8: Candidate points proposed by Ansys software using MISQP.

	Starting Point	CP 1	CP 2	CP3
P1-Spacing (mm)	120.00	107.70	104.00	101.00
P2-HeightTube (mm)	50.00	72.54	67.53	64.43
P3-ThTubeLayer (mm)	100.00	84.90	88.32	90.38
P5-ThSurfaceLayer (mm)	12.00	8.95	9.67	10.10
P6-ExtD (mm)	20.00	23.04	22.34	21.92
P7-ThTube (mm)	2.00	1.005	1.12	1.30
P8-Surface temperature (°C)	26.93	29.00	28.51	28.18
Variation from reference (%)	0.00	7.70	6.86	4.66
P9-Surface heat flux (W/m^2)	108.50	142.10	134.20	129.00
Variation from reference (%)	0.00	30.94	23.64	18.89

5.4.4 Results Compilation

After getting all these results, to better visualize the different possibilities of geometries and their corresponding results, tables and images corresponding to the solutions are present in this section.

As it can be seen in Table 5.9, ASO is the method which gave the worst results but at the same time it is the one which took the least amount of time to converge into a solution.

NLPQL and MISQP algorithms both gave the same results when it comes to the heat flux and surface temperature, the difference is the value of the geometrical parameters.

Table 5.9: Best points resulting from all algorithms.

	Starting Point	ASO	NLPQL	MISQP
P1-Spacing (mm)	120.00	114.70	102.1	107.70
P2-HeightTube (mm)	50.00	45.00	72.18	72.54
P3-ThTubeLayer (mm)	100.00	82.00	85.75	84.90
P5-ThSurfaceLayer (mm)	12.00	8.27	8.30	8.95
P6-ExtD (mm)	20.00	20.93	20.92	23.04
P7-ThTube (mm)	2.00	1.15	1.31	1.01
P8-Surface temperature (°C)	26.93	28.14	29.00	29.00
Variation from reference (%)	0.00	4.49	7.68	7.68
P9-Surface heat flux (W/m^2)	108.50	128.20	142.10	142.10
Variation from reference (%)	0.00	18.16	30.97	30.97

The geometry of the best ASO radiant floor system is present in Figure 5.18, the geometry of the best NLPQL radiant floor system is present in Figure 5.19 and the geometry of the best MISQP radiant floor system is present in Figure 5.20. NLPQL and MISQP being better optimization algorithms provided similar solutions, better than ASO. The objective function is to maximize heat flux so the tubing becomes bigger and closer to each other, as well as the distance to the surface being smaller. The dimensional constraints are put in place so the components of the system have dimensions that make sense in the context of the real world. The constraint of surface temperature is also put in place, that is why the dimensions did not reach the upper or lower limit of their constraints.

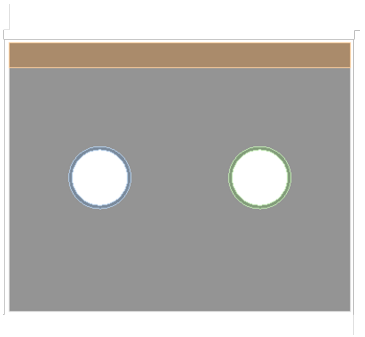

Figure 5.18: Geometry of the ASO model.

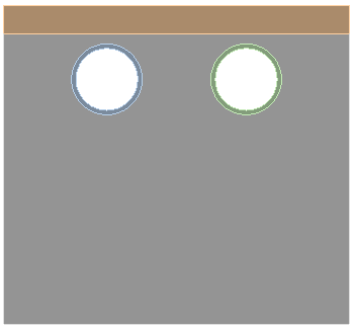

Figure 5.19: Geometry of the NLPQL model.

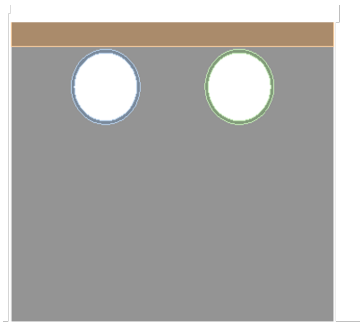

Figure 5.20: Geometry of the MISQP model.

As it can be seen by these figures, there is a big variety of different options for the geometry of the radiant floor system, the NLPQL and MISQP model provide the same values for the outputs but their geometries are different from one another, proving that different geometries can have the same outputs.

The designer of the radiant floor system has to choose which variables matter the most and then find the best combination for each individual case of installation of a

system.

Figure 5.21 shows the temperature distribution of the ASO system, Figure 5.22 shows the temperature distribution of the NLPQL system and Figure 5.23 shows the temperature distribution of the MISQP system.

The behavior inside the models is different from one another due to their differences in the geometry. For the case of the ASO model, the surface temperature is the lowest, NLPQL and MISQP models provide almost the same value of surface temperature with NLPQL being superior by a few decimals.

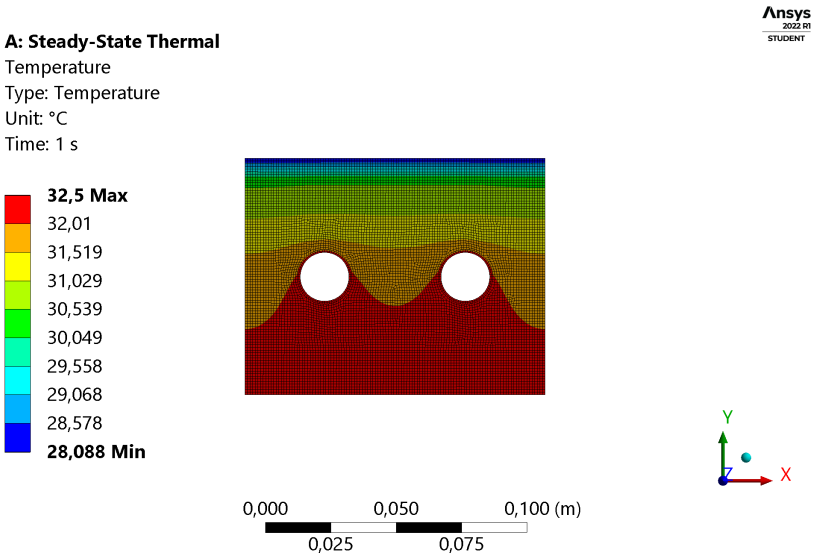

Figure 5.21: Temperature Distribution of the ASO Radiant floor system.

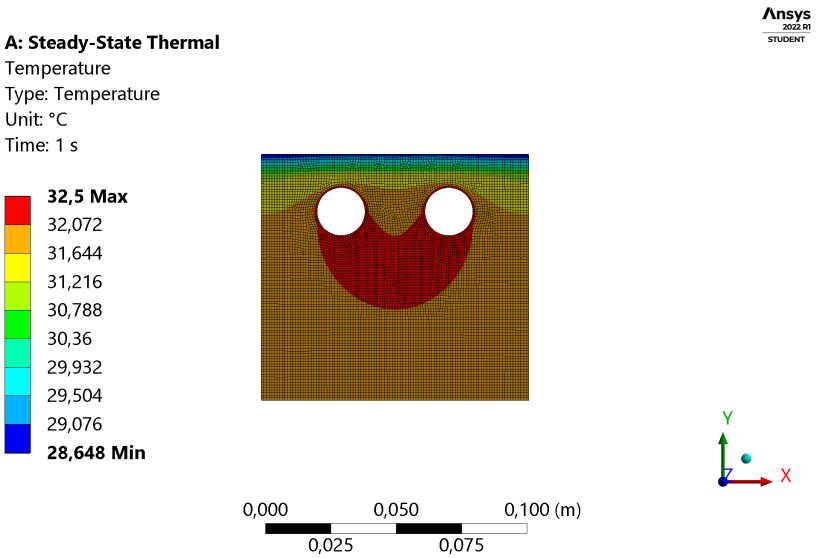

Figure 5.22: Temperature Distribution of the NLPQL Radiant floor system.

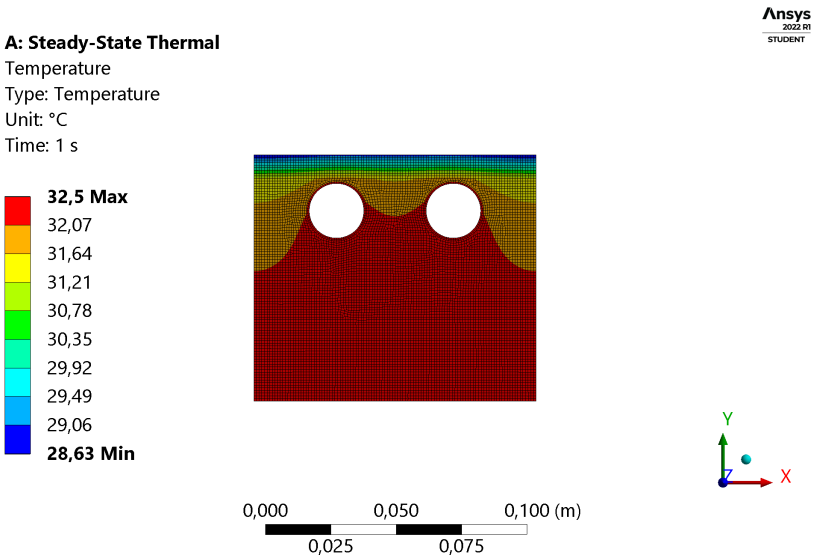

Figure 5.23: Temperature distribution of the MISQP radiant floor system.

Figure 5.24 shows the heat flux distribution of the ASO system, Figure 5.25 shows the heat flux distribution of the NLPQL system and Figure 5.26 shows the heat flux distribution of the MISQP system. All these systems have different heat distributions throughout their bodies because of their different geometries. From all these systems ASO provides the lowest heat flux value, and the MISQP and NLPQL provide similar highest values.

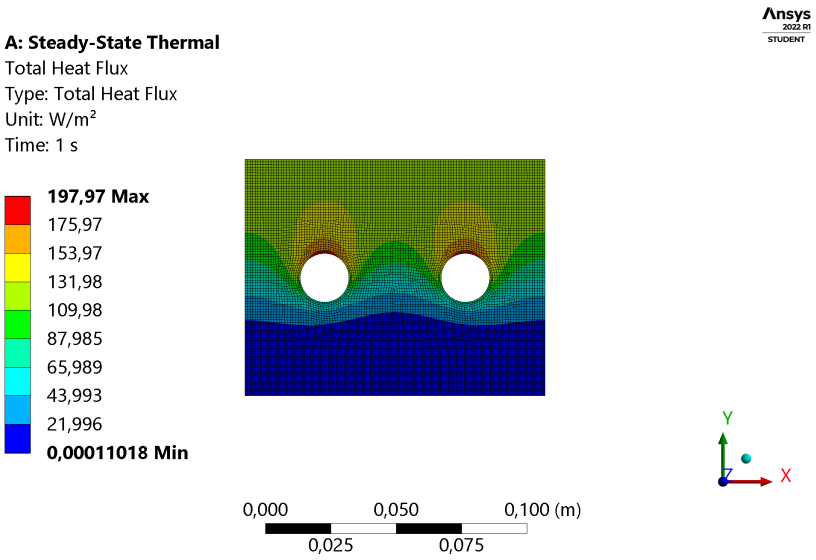

Figure 5.24: Heat flux distribution of the ASO radiant floor system.

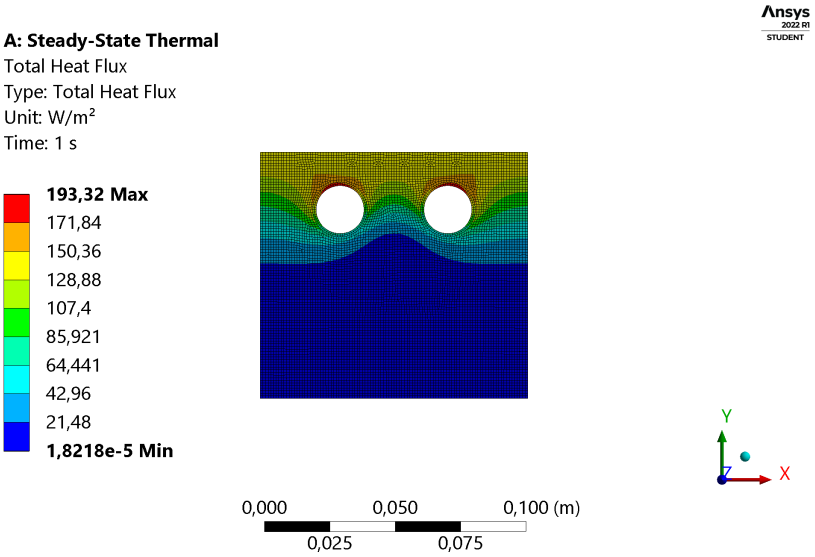

Figure 5.25: Heat flux distribution of the NLPQL radiant floor system.

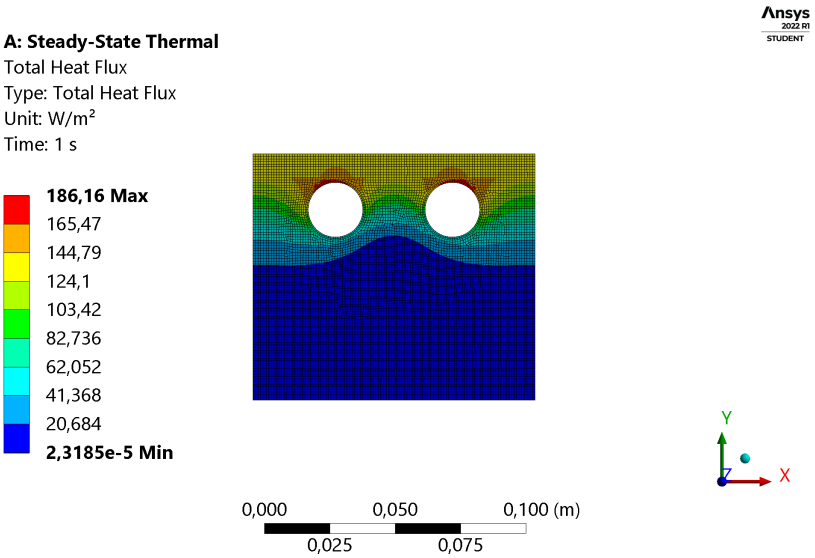

Figure 5.26: Heat flux distribution of the MISQP radiant floor system.

Overall, from the standard model, the optimization algorithms provided by Ansys were able to improve the heat flux output from 108.50 W/m^2 to 142.10 W/m^2, an improvement of 30.97%.

This final optimized model can be seen in Figure 5.27, with its respective geometrical parameters in millimeters. Compared to the original setup, it can be seen that this setup has its tubing very close to one another and really close to the surface. This result supports that there is a big importance of the distance between the tubing and distance from the tubing to the surface.

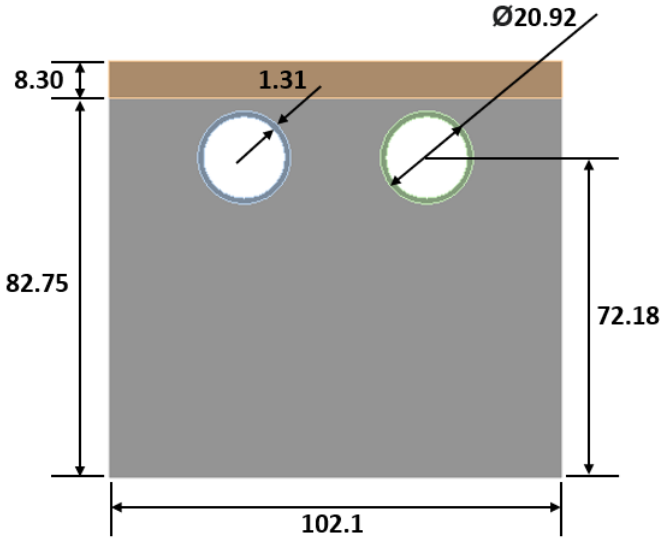

Figure 5.27: Configuration of the optimized model.

Intentionally blank page.

Chapter 6

Final Remarks

6.1 Conclusions

To conclude, by researching and carrying out a sensitivity analysis of the analytical equations found to support this study, the most important variables to take into account the design of a radiant floor system are:

- Distance of the piping to the surface of the floor;
- Spacing between the tubes;
- Thickness of the multiple layers, with special attention to the layer that the tubes are embedded into.

Performing the optimization of a system in Excel also proved to be a great method to reach an optimized solution, using GRG Nonlinear and Evolutionary optimization algorithms. Comparing these two algorithms evolutionary is more robust and slower than GRG Nonlinear.

Numerical analysis of the process using ANSYS helps to accurately predict the temperature distribution and heat flux output in the surface region throughout this work.

In this dissertation a sensitivity analysis was performed to illustrate the influence of design parameters of a floor heating system on its performance. Finite element method was used for solution of a typical considered domain. Three heat transfer mechanisms; conduction, convection and radiation have been considered to operate in this domain. Based on the results it is concluded that different design parameters have different effects on performance of the floor heating system in a room. The most influential parameters after performing the numerical analysis are the ones with the highest sensitivity value:

- Thickness of the tubing layer;
- Thickness of the surface layer;
- Distance of the piping to the surface of the floor.

Optimization was performed using three different algorithms. Regarding the optimization algorithms, ASO is the least reliable algorithm, considering the candidate points obtained and the results of heat flux that is lower compared to the other two. At the same time, it is the one which requires less computer power, and is the fastest.

NLPQL and MISQP provided candidate point 1 with the same value of heat flux but with different input parameters. These algorithms are gradient based so they require more computer power and are much slower when compared to the first algorithm. Between both algorithms the slower was NLPQL due to needing 83 design points to reach convergence compared to the 72 design points of MISQP.

When compared to the non optimized radiant floor system, the best solution proposed has 30,94% higher heat flux and 7,70% higher surface temperature.

The best configuration is presented in table 6.1.

Table 6.1: Parameters of the best radiant floor system configuration.

	Optimized Point
P1-Spacing (mm)	102.10
P2-HeightTube (mm)	72.18
P3-ThTubeLayer (mm)	85.75
P5-ThSurfaceLayer (mm)	8.30
P6-ExtD (mm)	20.92
P7-ThTube (mm)	1.31
P8-Surface temperature (°C)	29.00
P9-Surface heat flux (W/m^2)	142.10

This type of optimization of a radiant floor system is very advantageous, for example, if a radiant floor system has to have a set of fix input parameters but can change the value of other input variables, a balance can be accomplished where the optimized solution can be reached using these different methods previously studied.

Additionally, knowing the necessary heat flux to heat a room, the best solution can be found taking into account all the different parameters and variables reaching an equilibrium without over-designing or under-designing the system.

6.2 Future Work

The next step for possible future work is: Carrying out an additional study in the subject of radiant floor systems using the previous parameters to study and test in an experimental setup.

The studied variables were the surface temperature of the floor and the heat flux output, but other variables can also be studied such as the PMV, and the thermal comfort indicators.

In this dissertation, mostly geometrical parameters were studied, a radiant floor system involves many other factors and components. Broadening the problem to not only the floor itself but to its components there is a possibility to study the effect of different room conditions, such as wall isolation on the performance and efficiency of the system. An important aspect is the heat source, this component can also be subject to optimization and study to improve the efficiency of the overall system.

The numerical analysis in this dissertation was made using 2D models. 3D models can also be done in the future to compare the results, with this third dimension further

study can be done when it comes to the optimization of the layout of the radiant floor system.

Moreover, to achieve the high-end performance, other variables in addition to the ones explored here should also be assessed in future work, such as water supply temperature and flow rate, and the energy storage capability that could be given to some of the system layers with the use of phase change materials.

Intentionally blank page.

Bibliography

[Agency 2018] Iea International Energy Agency. World Energy Outlook. `www.iea.org/weo`, 2018. Accessed: 2022-01-29.

[Akçaözoğlu *et al.* 2013] Semiha Akçaözoğlu, Kubilay Akçaözoğlu and Cengiz Duran Atiş. Thermal conductivity, compressive strength and ultrasonic wave velocity of cementitious composite containing waste PET lightweight aggregate (WPLA). *Composites Part B: Engineering*, 45(1):721–726, 2013.

[Alfano *et al.* 2014] Francesca Romana D'Ambrosio Alfano, Bjarne W. Olesen, Boris Igor Palella and Giuseppe Riccio. Thermal comfort: Design and assessment for energy saving. *Energy and Buildings*, 81:326–336, 2014.

[Athienitis 1997] Andreas K Athienitis. Investigation of thermal performance of a passive solar building with floor radiant heating. *Solar energy*, 61(5):337–345, 1997.

[Barati 2013] Reza Barati. Application of excel solver for parameter estimation of the nonlinear Muskingum models. *KSCE Journal of Civil Engineering*, 17:1139–1148, 7 2013.

[Bojić *et al.* 2013] Milorad Bojić, Dragan Cvetković, Vesna Marjanović, Mirko Blagojević and Zorica Djordjević. Performances of low temperature radiant heating systems. *Energy and Buildings*, 61:233–238, 2013.

[Bozkir and Canbazoğlu 2004] Oğuz G. Bozkir and Suat Canbazoğlu. Unsteady thermal performance analysis of a room with serial and parallel duct radiant floor heating system using hot airflow. *Energy and Buildings*, 36:579–586, 6 2004.

[by Danfoss 2022] Devi by Danfoss. Indoor Cable Floor Heating Systems Application Manual. `https://devi.danfoss.com/media/1764/devi_indoors_vgluh102.pdf`, 2022.

[Chen and Li 2021] Qiong Chen and Nan Li. Fast simulation and high-fidelity reduced-order model of the multi-zone radiant floor system for efficient application to model predictive control. *Energy and Buildings*, 248:111210, 2021.

[Department of Energy *et al.* 2011] US Department of Energy et al. Buildings energy data book. *Energy Efficiency & Renewable Energy Department*, 286, 2011.

[Exploration 2013] ANSYS Design Exploration. ANSYS Design Exploration User's Guide Release 15.0. *ANSYS Inc*, 2013.

[González and Prieto 2021] B. González and M.M. Prieto. Radiant heating floors with PCM bands for thermal energy storage: A numerical analysis. *International Journal of Thermal Sciences*, 162:106803, 2021.

[Grebenişan and Salem 2017] Gavril Grebenişan and Nazzal Salem. The multi-objective genetic algorithm optimization, of a superplastic forming process, using ansys®. Vol. 126. EDP Sciences, 10 2017.

[Gwerder *et al.* 2008] M. Gwerder, B. Lehmann, J. Tödtli, V. Dorer and F. Renggli. Control of thermally-activated building systems (TABS). *Applied Energy*, 85:565–581, 2008.

[Hasan *et al.* 2009] Ala Hasan, Jarek Kurnitski and Kai Jokiranta. A combined low temperature water heating system consisting of radiators and floor heating. *Energy and Buildings*, 41:470–479, 5 2009.

[Hashemi *et al.* 2020] Seyed Hossein Hashemi, Seyed Ali Mousavi Dehghani, Seyed Ehsan Samimi, Mahmood Dinmohammad and Seyed Abdolrasoul Hashemi. Performance comparison of GRG algorithm with evolutionary algorithms in an aqueous electrolyte system. *Modeling Earth Systems and Environment*, 6:2103–2110, 12 2020.

[ISO 2005] ISO. ISO 7730:2005 ergonomics of the thermal environment-Analytical determination and interpretation of thermal comfort using calculation of the PMV and PPD indices and local thermal comfort criteria., 2005.

[ISO 2012] ISO. ISO 11855e1:2012(E) building environment design-Design, dimensioning, installation and control of embedded radiant heating and cooling systems. Part 1: definition, sysmbols, and comfort criteria. 2012., 2012.

[Jin *et al.* 2010] Xing Jin, Xiaosong Zhang and Yajun Luo. A calculation method for the floor surface temperature in radiant floor system. *Energy and Buildings*, 42:1753–1758, 10 2010.

[Joe and Karava 2019] Jaewan Joe and Panagiota Karava. A model predictive control strategy to optimize the performance of radiant floor heating and cooling systems in office buildings. *Applied Energy*, 245:65–77, 7 2019.

[John Siegenthaler 2012] P.E. John Siegenthaler. Modern Hydronic Heating For Residential and Ligh Commercial Buildings, 3e. Delmar, Cengage Learning, 2012.

[Khuri and Mukhopadhyay 2010] André I Khuri and Siuli Mukhopadhyay. Response surface methodology. *Wiley Interdisciplinary Reviews: Computational Statistics*, 2(2):128–149, 2010.

[Kong *et al.* 2017] Qiongxiang Kong, Ji Feng, Chunlei Yang, Zhen Miao and Xiao He. Numerical Simulation of a Radiant Floor Cooling Office Based on CFD-BES Coupling and FEM. *Energy Procedia*, 105:3577–3583, 2017. 8th International Conference on Applied Energy, ICAE2016, 8-11 October 2016, Beijing, China.

[Koschwitz *et al.* 2018] D. Koschwitz, J. Frisch and C. van Treeck. Data-driven heating and cooling load predictions for non-residential buildings based on support vector machine regression and NARX Recurrent Neural Network: A comparative study on district scale. *Energy*, 165:134–142, 2018.

[Laouadi 2004] Abdelaziz Laouadi. Development of a radiant heating and cooling model for building energy simulation software. *Building and Environment*, 39:421–431, 2004.

[Lehmann *et al.* 2011] B. Lehmann, V. Dorer, M. Gwerder, F. Renggli and J. Tödtli. Thermally activated building systems (TABS): Energy efficiency as a function of control strategy, hydronic circuit topology and (cold) generation system. *Applied Energy*, 88:180–191, 2011.

[Liu *et al.* 2015] Zhongbing Liu, Ling Zhang, Guangcai Gong, Yongqiang Luo and Fangfang Meng. Evaluation of a prototype active solar thermoelectric radiant wall system in winter conditions. *Applied Thermal Engineering*, 89:36–43, 6 2015.

[Liu *et al.* 2020] Jiying Liu, Xuwei Zhu, Moon Keun Kim, Ping Cui, Shengwei Zhu and Risto Kosonen. A Transient Two-dimensional CFD Evaluation of Indoor Thermal Comfort with an Intermittently-operated Radiant Floor Heating System in an Office Building. 7:62–87, Dec. 2020.

[Ma *et al.* 2013] Peizheng Ma, Lin-Shu Wang and Nianhua Guo. Modeling of TABS-based thermally manageable buildings in Simulink. *Applied Energy*, 104:791–800, 2013.

[Menon 2005] Ajaykumar Menon. Structural optimization using ANSYS and regulated multiquadric response surface model. 2005.

[Meyghani *et al.* 2017] Bahman Meyghani, Mokhtar B. Awang, Seyed Sattar Emamian, Mohd Khalid B. Mohd Nor and Srinivasa Rao Pedapati. A comparison of different finite element methods in the thermal analysis of friction stir welding (FSW). *Metals*, 7, 10 2017.

[Olesen 2012] Bjarne Olesen. Thermo Active Building Systems Using Building Mass To Heat and Cool. *Ashrae Journal*, 54:44–+, 02 2012.

[Park *et al.* 2014] Sang Hoon Park, Woong June Chung, Myoung Souk Yeo and Kwang Woo Kim. Evaluation of the thermal performance of a Thermally Activated Building System (TABS) according to the thermal load in a residential building. *Energy and Buildings*, 73:69–82, 4 2014.

[Qiu and Li 2011] Lin Qiu and Qiang Li. Analyses on two paving types of floor heating. *Proceedings - International Conference on Computer Distributed Control and Intelligent Environmental Monitoring, CDCIEM 2011*, pp. 1431–1433, 2011.

[Rhee *et al.* 2017] Kyu Nam Rhee, Bjarne W. Olesen and Kwang Woo Kim. Ten questions about radiant heating and cooling systems. *Building and Environment*, 112:367–381, 2 2017.

[Richard Watson 2004] Kirby Chapman Richard Watson. Radiant heating and cooling handbook. McGraw-Hill, 2004.

[Romaní *et al.* 2016] Joaquim Romaní, Alvaro De Gracia and Luisa F. Cabeza. Simulation and control of thermally activated building systems (TABS). *Energy and Buildings*, 127:22–42, 9 2016.

[Ryu *et al.* 2004] Seong Ryong Ryu, Jae Han Lim, Myoung Souk Yeo and Kwang Woo Kim. A Study on the control methods for radiant floor heating and cooling system in residential building. *ASHRAE Transactions*, 110 PART II:106–116, 2004. null ; Conference date: 26-06-2004 Through 30-06-2004.

[Rüdisser 2017] Daniel Rüdisser. Dynamic simulation and comparison of two underfloor heating systems. `https://www.htflux.com/en/dynamic-simulation-and-comparison-of-two-underfloor-heating-systems/`, 2017. Accessed: 2022-05-26.

[Salem 2017] Nazzal Salem. Parameterized Finite Element Analysis With Optimization of a Superplastic Forming Process Using ANSYS®. pp. 319–332, 2017.

[Sattari and Farhanieh 2006] S. Sattari and B. Farhanieh. A parametric study on radiant floor heating system performance. *Renewable Energy*, 31(10):1617–1626, 2006.

[Schmelas *et al.* 2015] Martin Schmelas, Thomas Feldmann and Elmar Bollin. Adaptive predictive control of thermo-active building systems (TABS) based on a multiple regression algorithm. *Energy and Buildings*, 103:14–28, 7 2015.

[Shin *et al.* 2015] Mi Su Shin, Kyu Nam Rhee, Seong Ryong Ryu, Myoung Souk Yeo and Kwang Woo Kim. Design of radiant floor heating panel in view of floor surface temperatures. *Building and Environment*, 92:559–577, 10 2015.

[Shukla *et al.* 2020] Saunak Shukla, Reza Daneshazarian, Aggrey Mwesigye, Wey H. Leong and Seth B. Dworkin. A novel radiant floor system: Detailed characterization and comparison with traditional radiant systems. *International Journal of Green Energy*, 17:137–148, 1 2020.

[Somassoundirame and Nithiyananthan 2021] Ramechecandane Somassoundirame and Eswari Nithiyananthan. Optimization of insulation on subsea oil and gas equipment. *Journal of Petroleum Exploration and Production*, 11:1007–1018, 2 2021.

[Thomas *et al.* 2011] Sébastien Thomas, Pierre Yves Franck and Philippe André. Model validation of a dynamic embedded water base surface heat emitting system for buildings. *Building Simulation*, 4:41–48, 3 2011.

[Verbeke and Audenaert 2018] Stijn Verbeke and Amaryllis Audenaert. Thermal inertia in buildings: A review of impacts across climate and building use. *Renewable and Sustainable Energy Reviews*, 82:2300–2318, 2 2018.

[Weitzmann *et al.* 2005] Peter Weitzmann, Jesper Kragh, Peter Roots and Svend Svendsen. Modelling floor heating systems using a validated two-dimensional ground-coupled numerical model. *Building and Environment*, 40(2):153–163, 2005.

[Werner-Juszczuk 2018] Anna Justyna Werner-Juszczuk. Experimental and numerical investigation of lightweight floor heating with metallised polyethylene radiant sheet. *Energy and Buildings*, 177:23–32, 10 2018.

[Woodson 2010] R.D. Woodson. Radiant Floor Heating, Second Edition. McGraw-Hill Education, 2010.

[Wu *et al.* 2015] Xiaozhou Wu, Jianing Zhao, Bjarne W. Olesen, Lei Fang and Fenghao Wang. A new simplified model to calculate surface temperature and heat transfer of radiant floor heating and cooling systems. *Energy and Buildings*, 105:285–293, 2015.

[Zhang *et al.* 2012] Lun Zhang, Xiao Hua Liu and Yi Jiang. Simplified calculation for cooling/heating capacity, surface temperature distribution of radiant floor. *Energy and Buildings*, 55:397–404, 12 2012.

[Zhang *et al.* 2013] Dongliang Zhang, Ning Cai and Zijie Wang. Experimental and numerical analysis of lightweight radiant floor heating system. *Energy and Buildings*, 61:260–266, 2013.

[Zhao *et al.* 2014] Kang Zhao, Xiao-Hua Liu and Yi Jiang. Dynamic performance of water-based radiant floors during start-up and high-intensity solar radiation. *Solar Energy*, 101:232–244, 2014.

[Zhou *et al.* 2018] Zhihua Zhou, Chendong Wang, Xiuhao Sun, Feng Gao, Wei Feng and George Zillante. Heating energy saving potential from building envelope design and operation optimization in residential buildings: A case study in northern China. *Journal of Cleaner Production*, 174:413–423, 1 2018.